Euclid NIR detector characterization at JPL Precision Projector Laboratory

Chaz Shapiro (Jet Propulsion Laboratory, California Institute of Technology)

Eric Huff (Jet Propulsion Laboratory, California Institute of Technology)

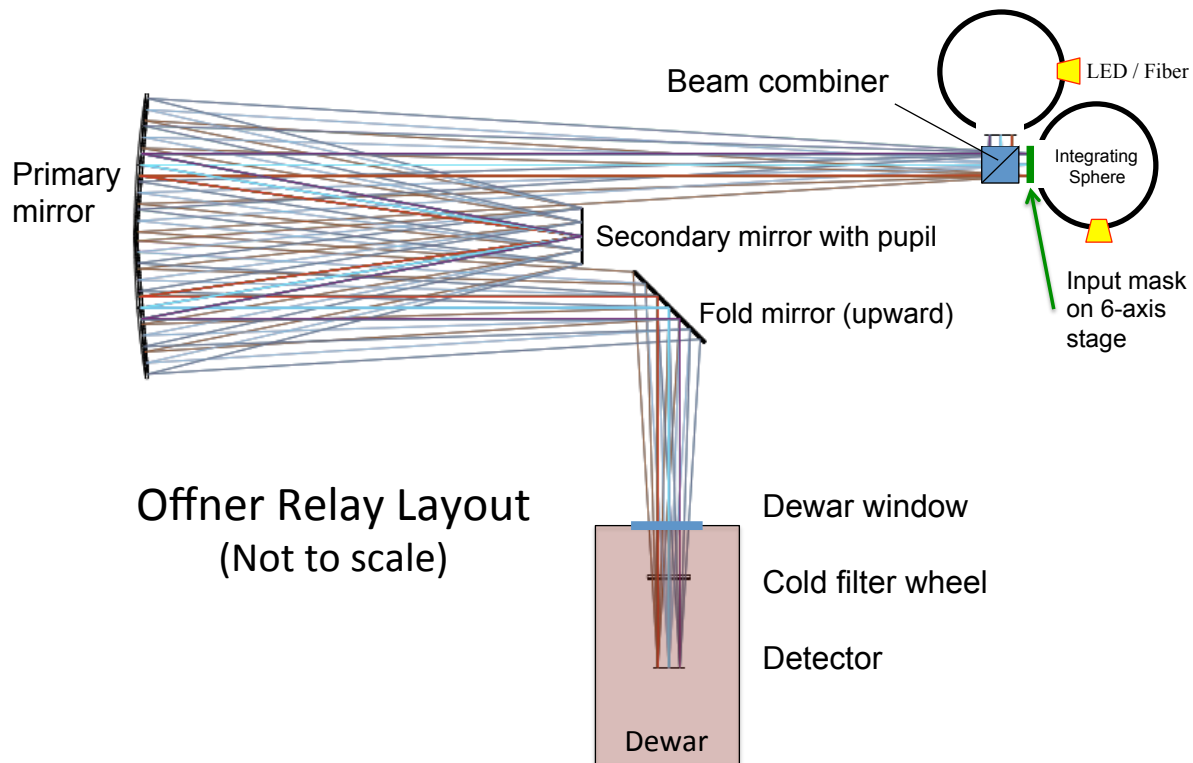Roger Smith (Caltech Optical Observatories)
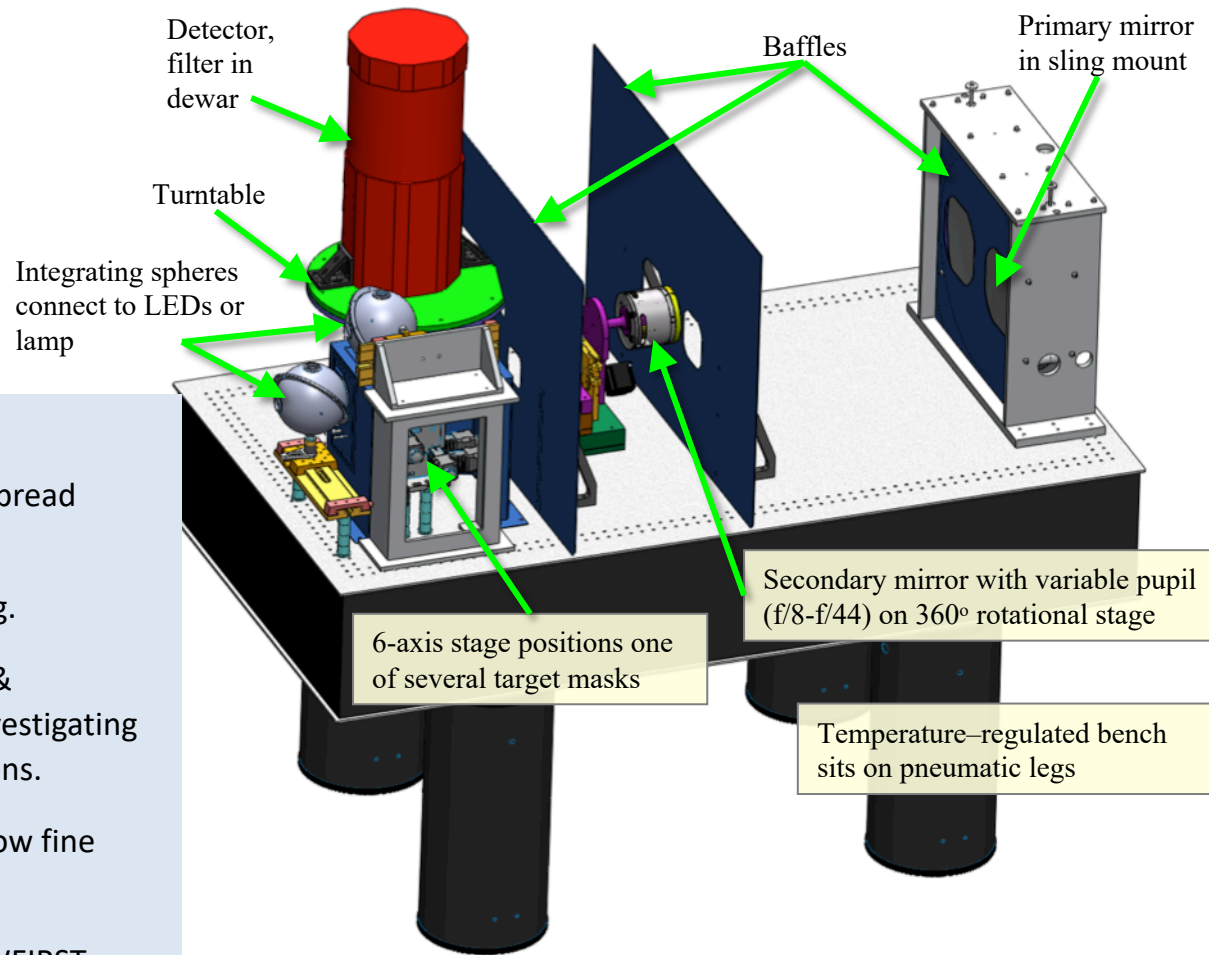
Andrés Plazas-Malagon (former Caltech)

Overview (spoilers)

- H2RG #18546 was loaned to Precision Projector Laboratory group at JPL/Caltech (thank you!)

- We emulated Euclid-like point source observations using our astronomical scene projector at 2 wavelengths (1µm, 1.55 µm)

- We find clear evidence for nonlinearity which depends on image contrast, including fluence-dependent PSF size (brighter-fatter effect)

- We find that the "crosshatch" pattern seen in flats is not entirely removed from photometry by flat-fielding, consistent with sub-pixel QE variations
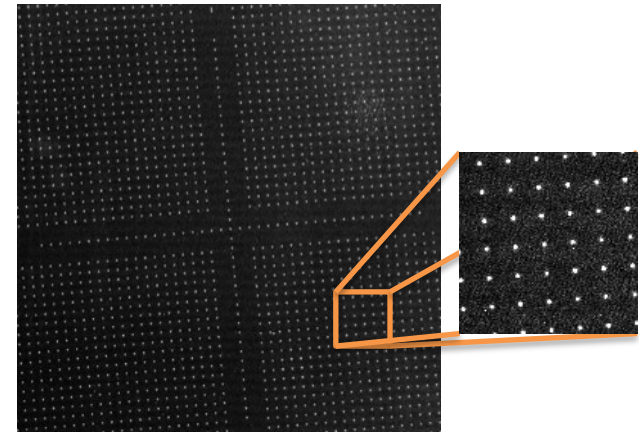
PPL Test-bed: "The Projector"

Beam combiner

LED / Fiber

Integrating
Sphere

Primary
mirror

Secondary mirror with pupil

Input mask
on 6-axis
stage

Fold mirror (upward)

Offner Relay Layout
(Not to scale)

Dewar window

Cold filter wheel

Detector

Dewar

Precision Projector Laboratory testbed

Projector System Features:

- Diffraction-limited optics with simple point spread function (PSF).

- High image stability through passive damping.

- Custom image masks, adjustable f/#, stages & illumination provide a range of signals for investigating various detector effects and mission conditions.

- Servo controls on mask and tip-tilt mirror allow fine image positioning for dithering or scanning.

- IMage COMbination algorithm implements WFIRST image reconstruction strategy with dithered, undersampled images.

- Dedicated 144 core cluster allows near real-time analysis of 1000's of images.

- **Projecting many sources simultaneously allows rapid characterization of an entire detector, averaging to detect weak effects, statistical analysis instead of analysis of isolated regions**

Detector, filter in dewar

Baffles

Primary mirror in sling mount

Turntable

Integrating spheres connect to LEDs or lamp

6-axis stage positions one of several target masks

Secondary mirror with variable pupil (f/8-f/44) on 360° rotational stage

Temperature–regulated bench sits on pneumatic legs
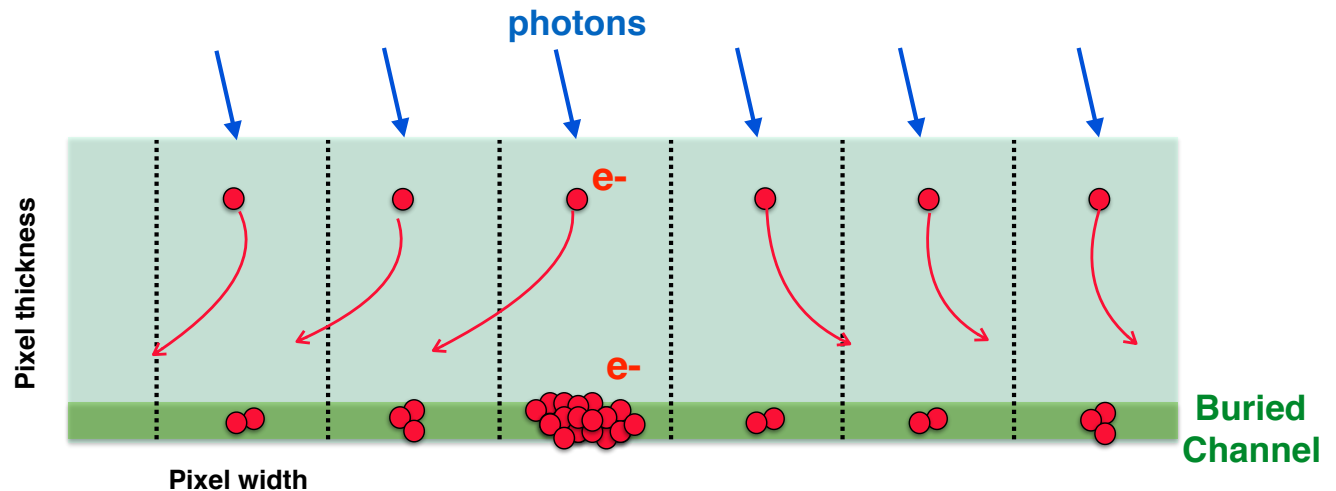
Image of 3μm spot grid (emulated stars)

The Brighter-fatter effect in CCDs

Inhomogenous distribution of the charges resulting from :
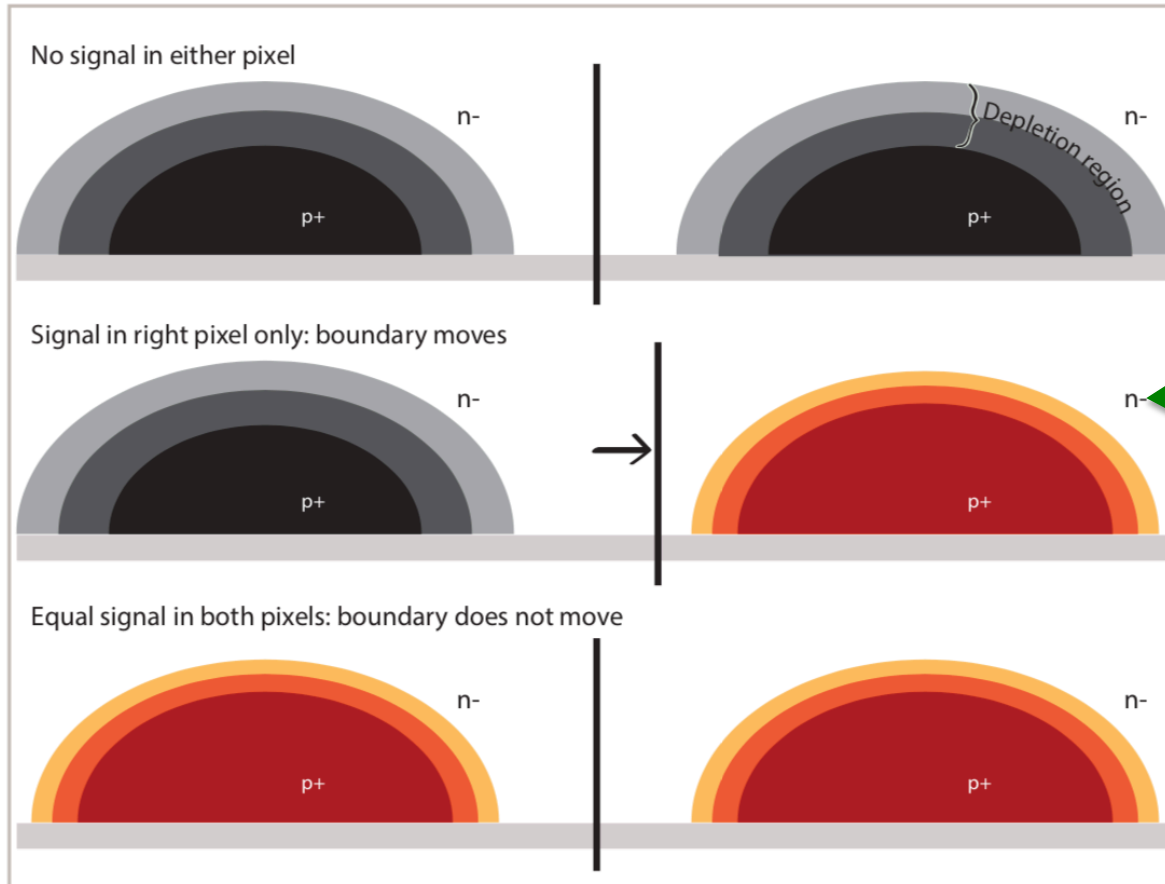
▷ Contrast from the photon noise in flatfield images.

▷ PSF of a star.

CCD model Image Credit:
Augustin Guyonnet

- BF has been seen in DECam, Megacam, LSST CCDs, HSC CCDs.

- Bad for weak lensing: misrepresentation of PSF model. DES: discard brightest stars to minimize impact on shear measurements (Jarvis et 2015, Zuntz et al. 2017).

The BF effect in HxRG detectors ??

No signal in either pixel

n-

Depletion region

n-

p+

p+

Signal in right pixel only: boundary moves

n-

n-

p+

p+

Equal signal in both pixels: boundary does not move

n-

n-

p+

p+

Photon detected

The effective pixel boundaries shift as pixels fill asymmetrically

Concept by Roger Smith; Image from **Plazas et al 2017**

Brighter-fatter test: data acquisition

- H2RG was cooled to 95K, operated by Leach controller at 166 kHz.

- A spot grid image (~18,000 spots) covers most of the detector. Spacing = 274.5µm = 15.25 pixels.

- **Using f/11 aperture and 1 (1.55) µm illumination**, the optical PSF width is 11 (17) µm. These are widened slightly by charge diffusion (σ=3µm) and lab seeing (σ=1µm)

- We "sample up the ramp" with 6 or 7 samples and average many (10-90) exposures of flat fields, spots, or darks. Reset frame is typically discarded.

- Burn-in/persistence allowed to reach steady state

- Calibrations applied to images: dark subtraction, conversion gain, pixel-wise nonlinearity, mean IPC, "bad" (outlier) pixels flagged,

- Identify spots with centroid < 0.1 pixels from a pixel center → average measurements over ~700 spots.
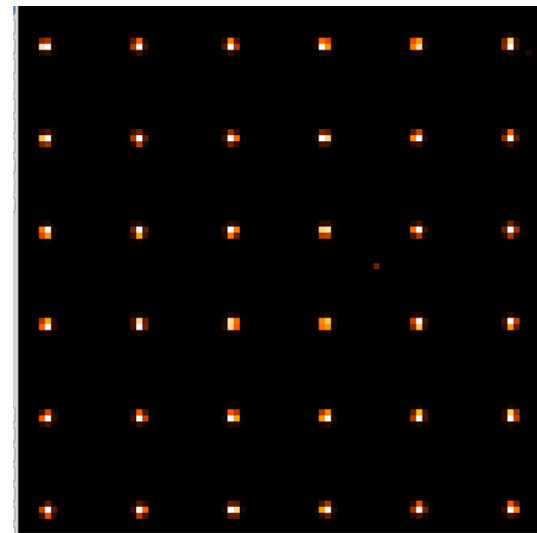
Median Y-band (1µm) spot

139 e^-/s (2,085 e^-)	522 e^-/s (7,826 e^-)	163 e^-/s (2,451 e^-)
532 e^-/s (7,976 e^-)	5048 e^-/s (77,5716 e^-)	521 e^-/s (7,812 e^-)
147 e^-/s (2,208 e^-)	521 e^-/s (7,812 e^-)	152 e^-/s (2,280 e^-)

Median profiles of ~700 centered spots

Exposures limited to ~50% full well
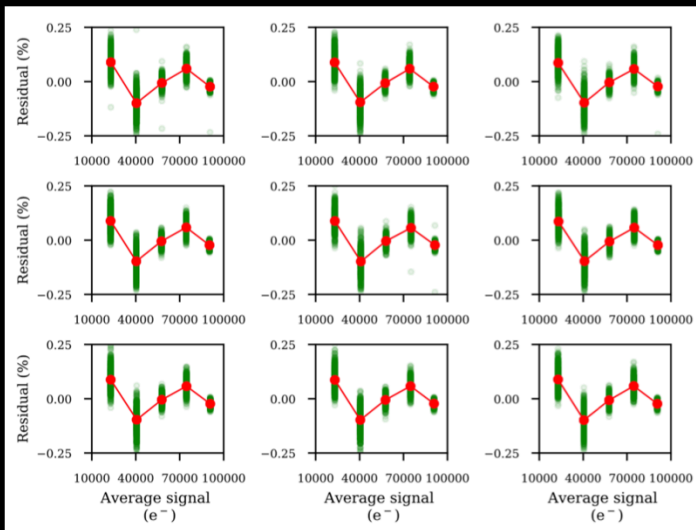
Y-band (1 µm)
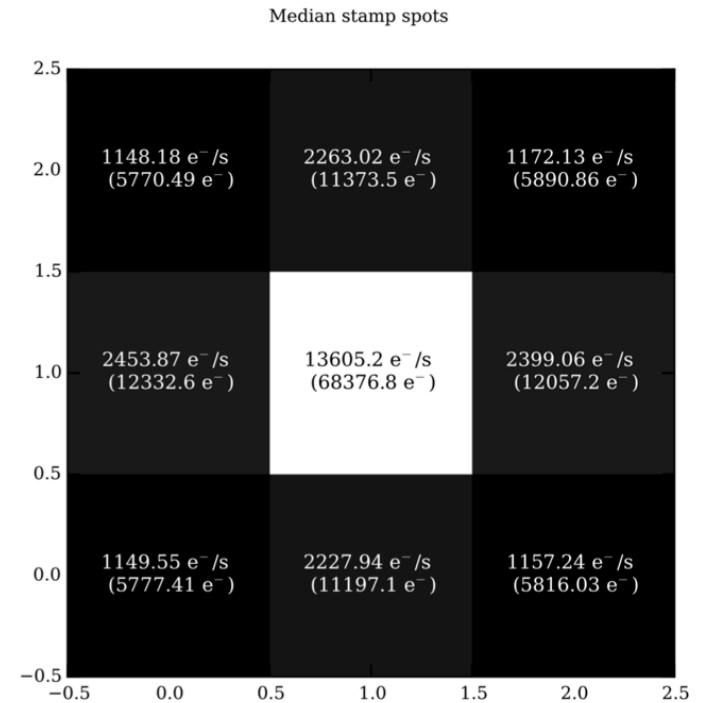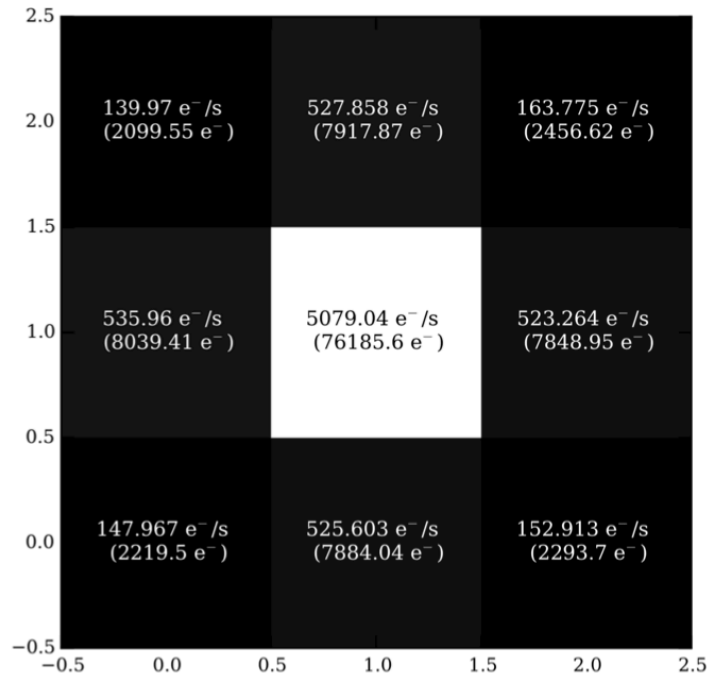
H-band (1.55 µm)

Center : Neighbor = 9.5 : 1

Center : Neighbor = 5.5 : 1

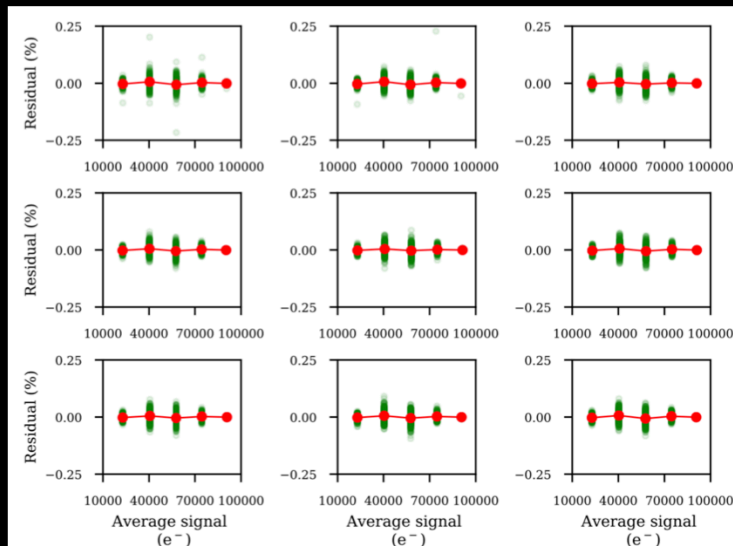(Wider spot, higher background)
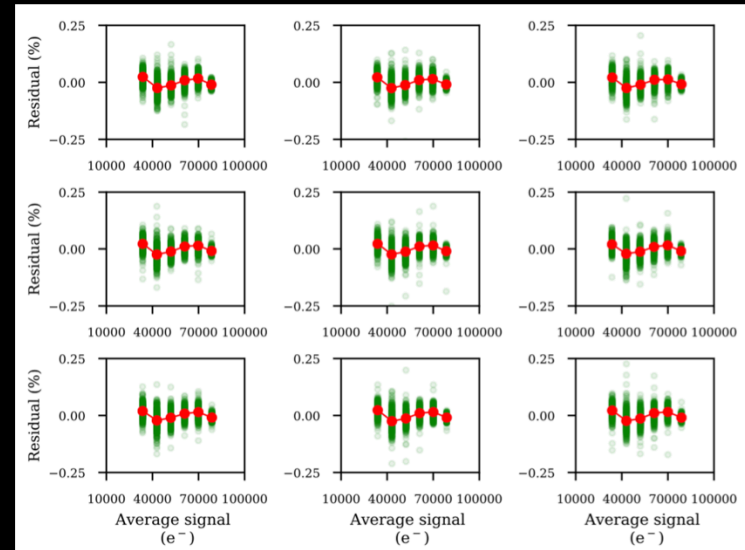
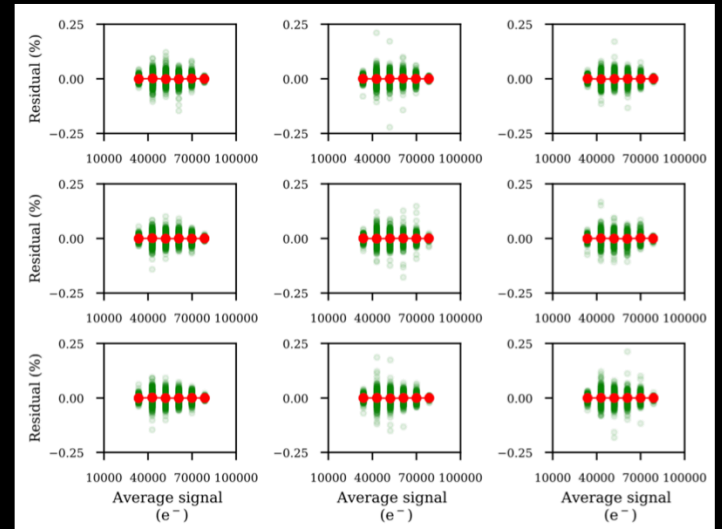# Residuals of nonlinearity correction w/ flats
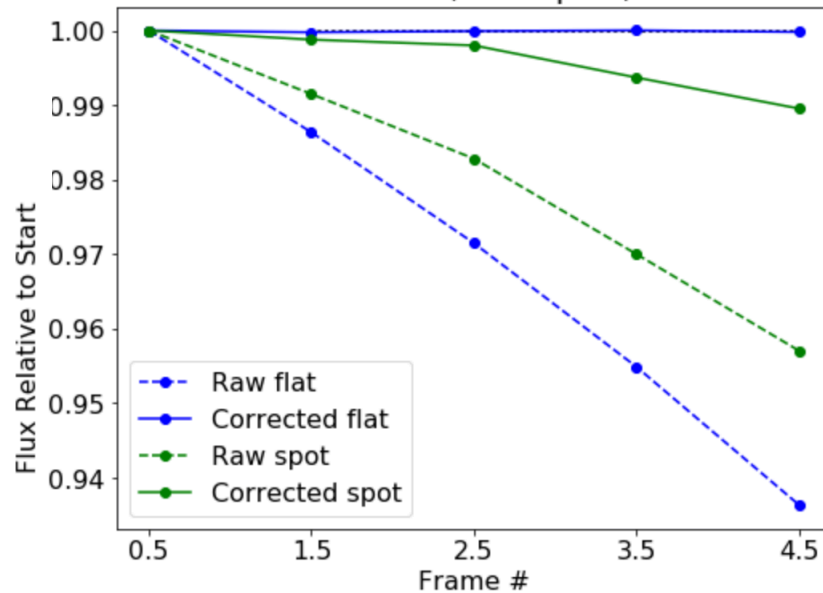

2nd order

Y-band (1 μm)

H-band (1.55 μm)

3rd order

Calibrated spot fluxes are not constant "up the ramp"

NL corrections are applied pixel-wise

Sums of 3x3 pixel regions
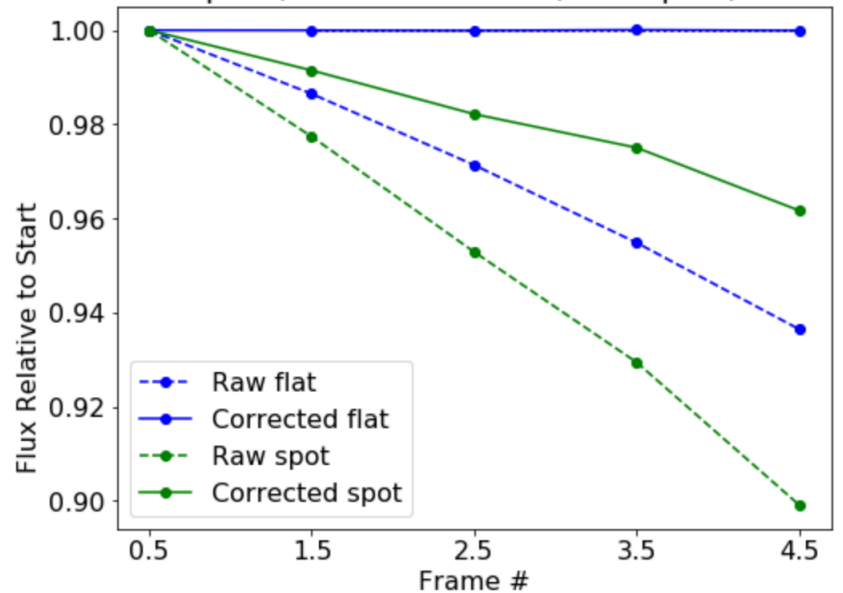
Fluxes computed by differencing sequential frames: "Frame 1.5" = Frame 1 – Frame 2

Calibrated spot fluxes are not constant "up the ramp"

As image integrates, neighbor pixels gain flux while center pixel loses flux

Y-band (1 μm)   H-band (1.55 μm)
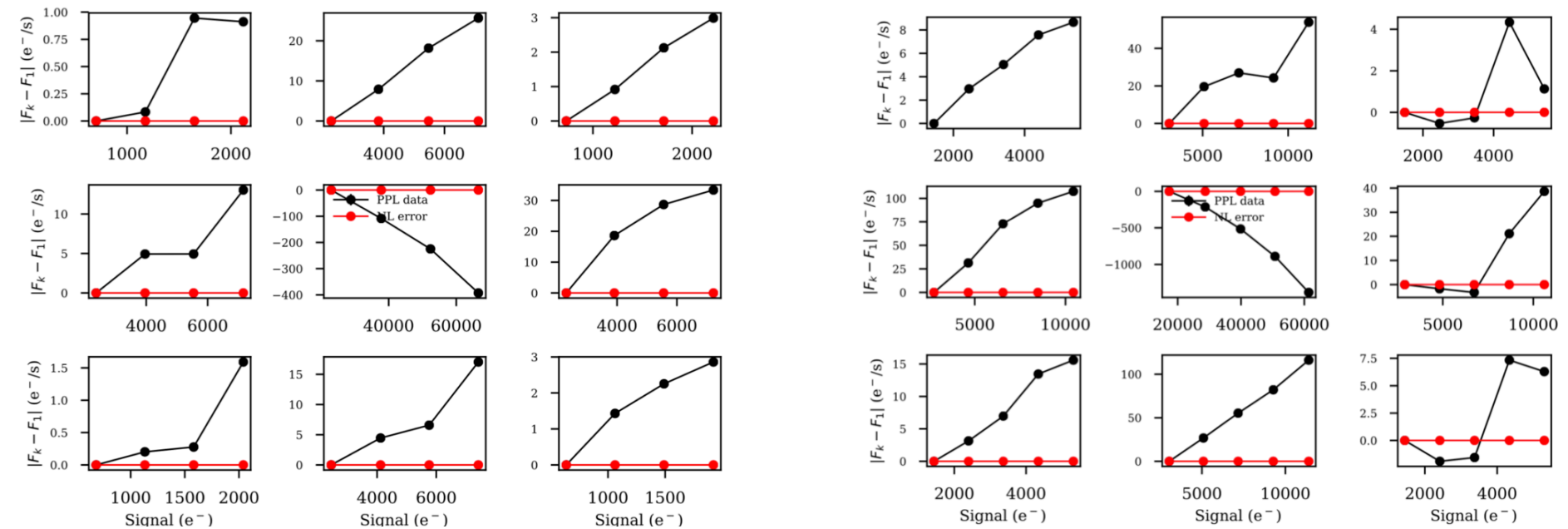
Black = data ; Red = propagation of NL residual

Calibrated spot fluxes are not constant "up the ramp"

Neighbor pixels do not balance loss of flux in center pixel

$$f_N = (F_i - F_1) \, / \, <\text{Total Spot Flux}>$$

Y-band (1 µm)
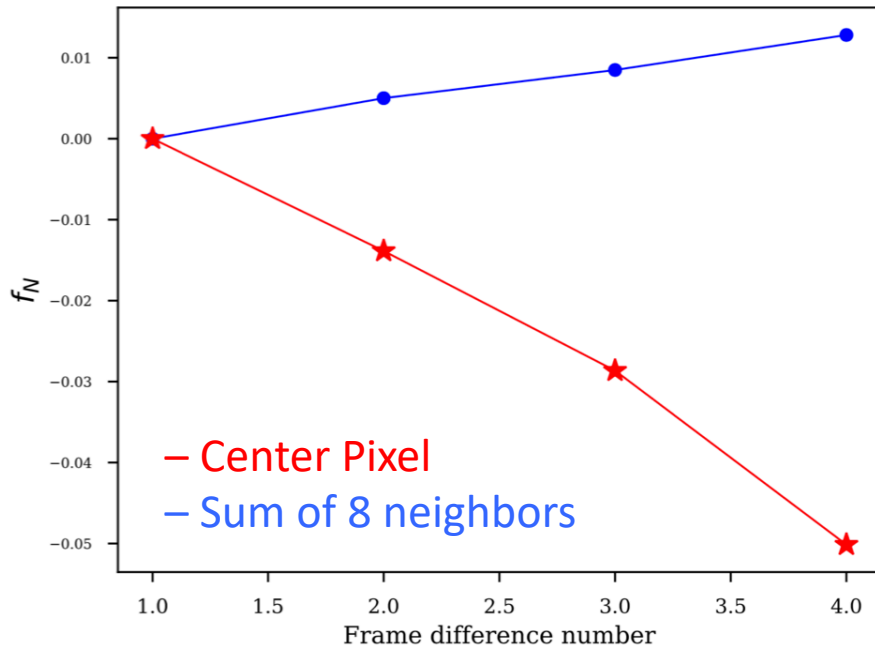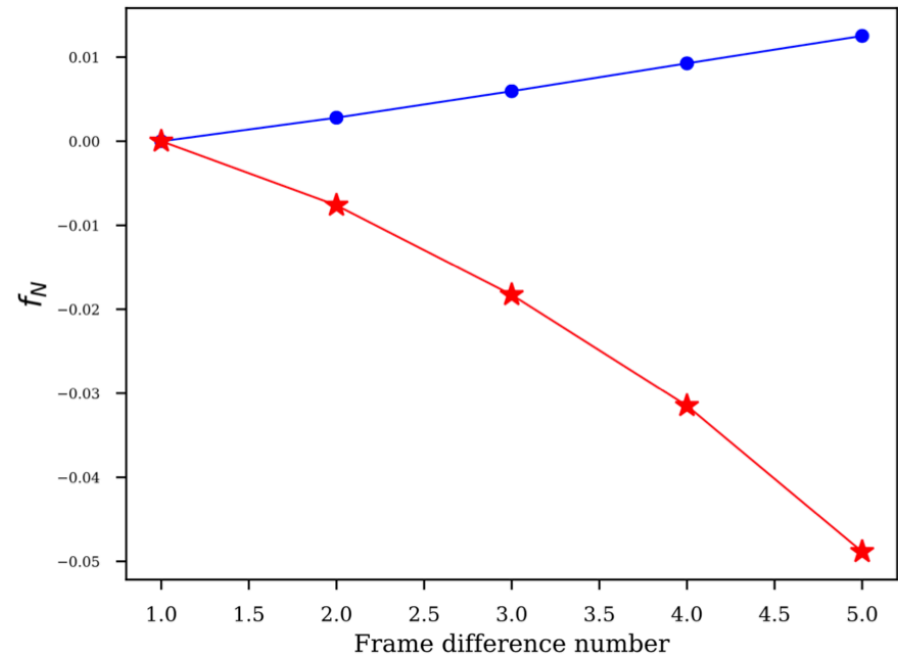
H-band (1.55 µm)

No effect seen on spots with centroids near pixel corners
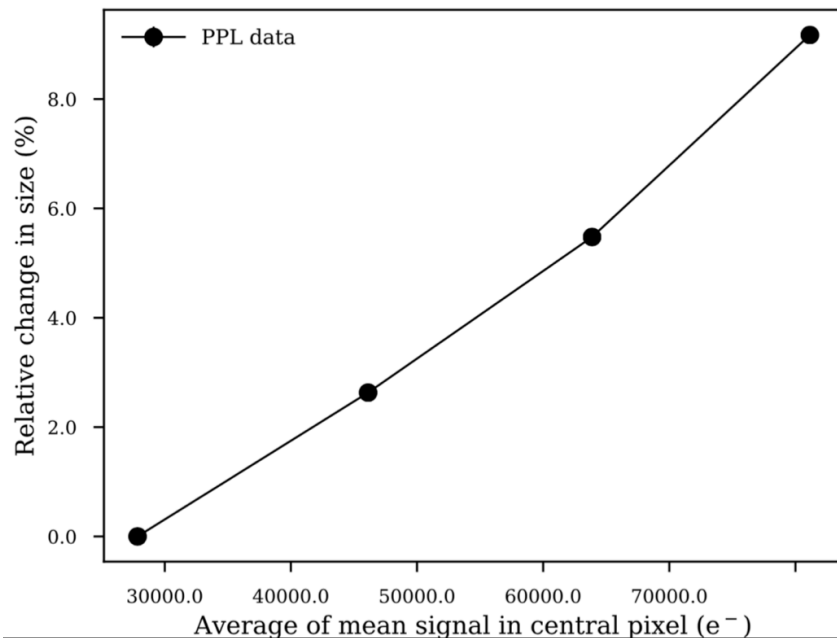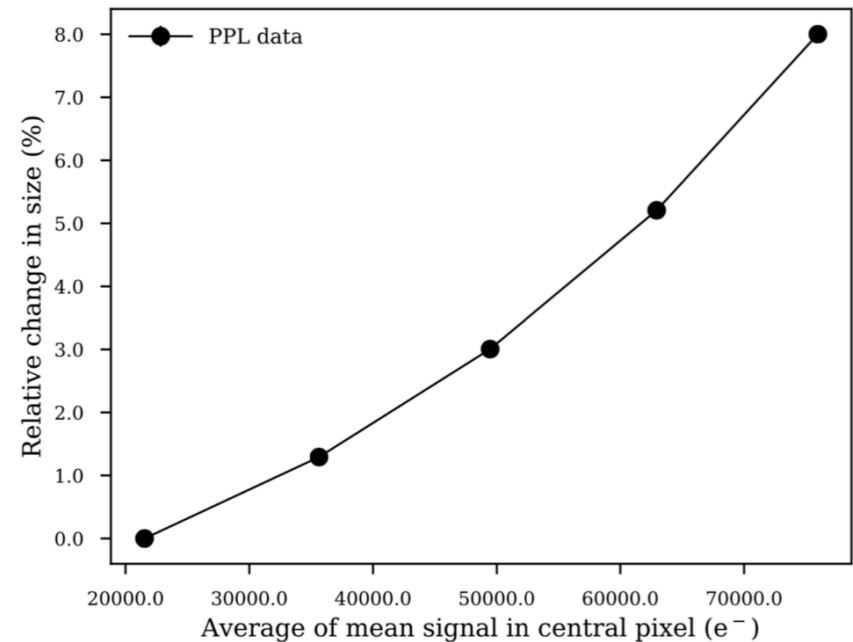
$$f_N = (F_i - F_1) / \text{<Total Spot Flux>}$$
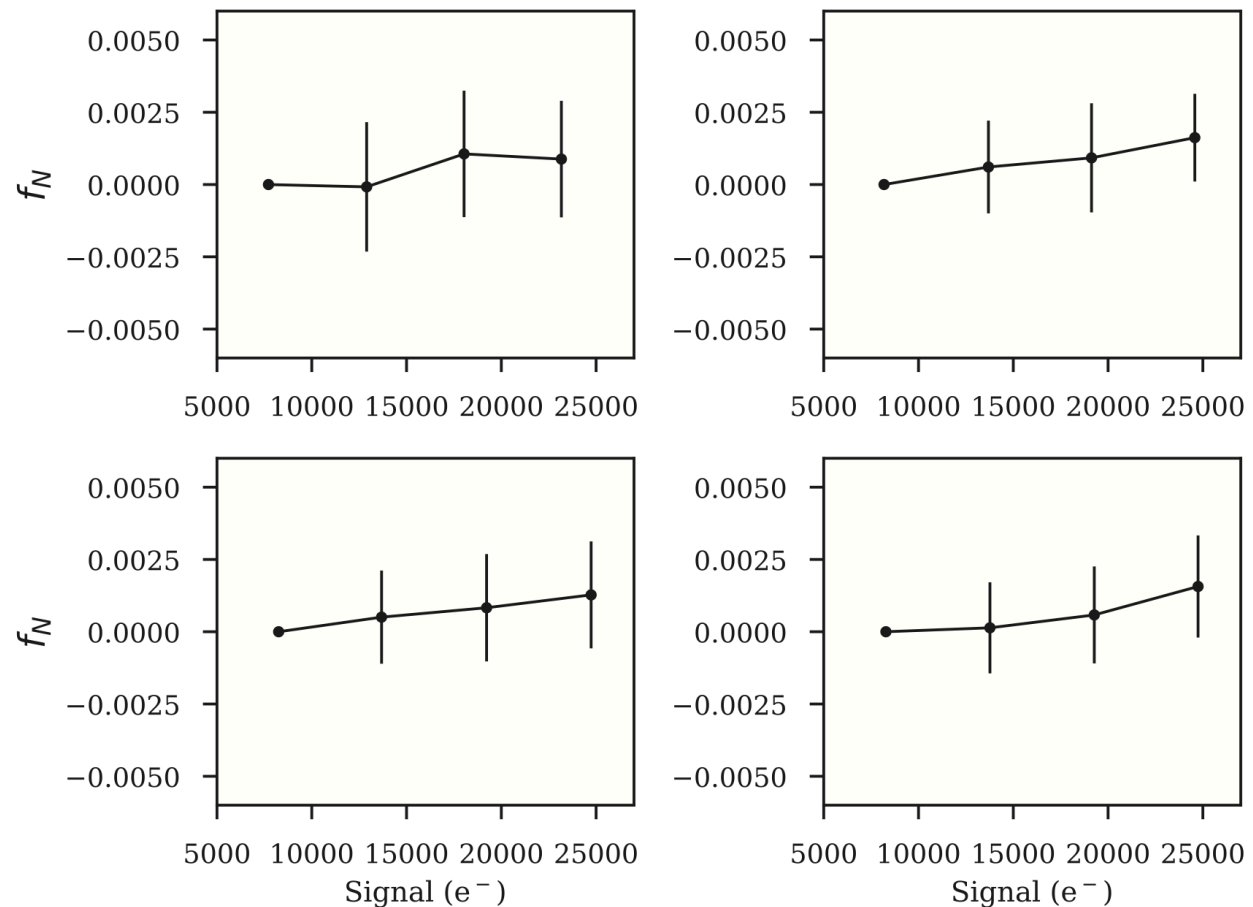
Y-band (1 µm)

Spot size change
(mostly driven by flux loss in center pixel)

Y-band (1 μm)

H-band (1.55 μm)

- "Size" = 2nd moment of PSF

- Effect is the same order of magnitude as Dark Energy Survey CCDs
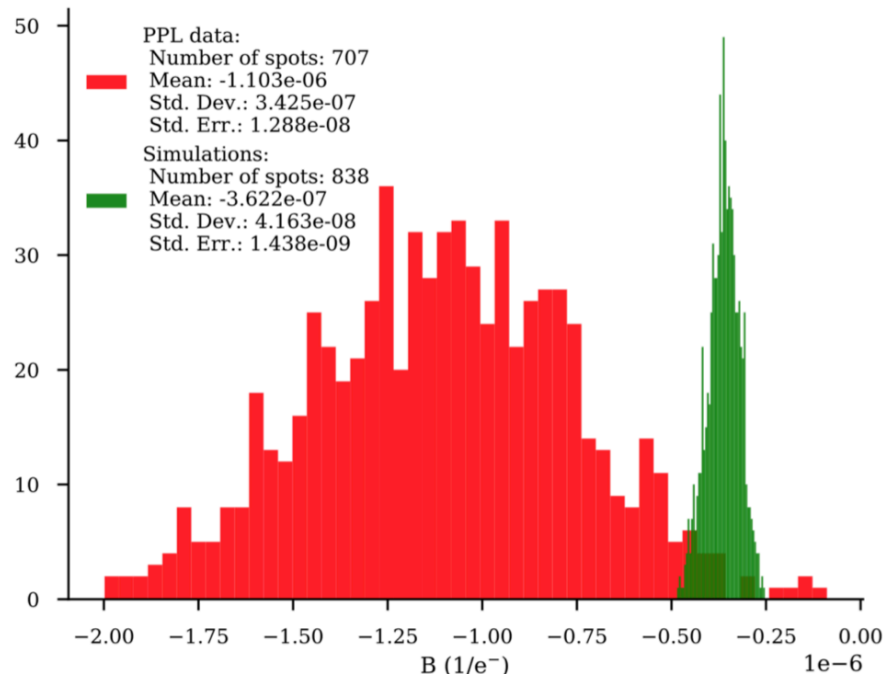
Estimating change in pixel area

Assumptions:
- Lost flux in center pixel is **entirely** due to pixel shrinking…
- Lost flux is uniformly distributed over center pixel (really it depends on PSF)…
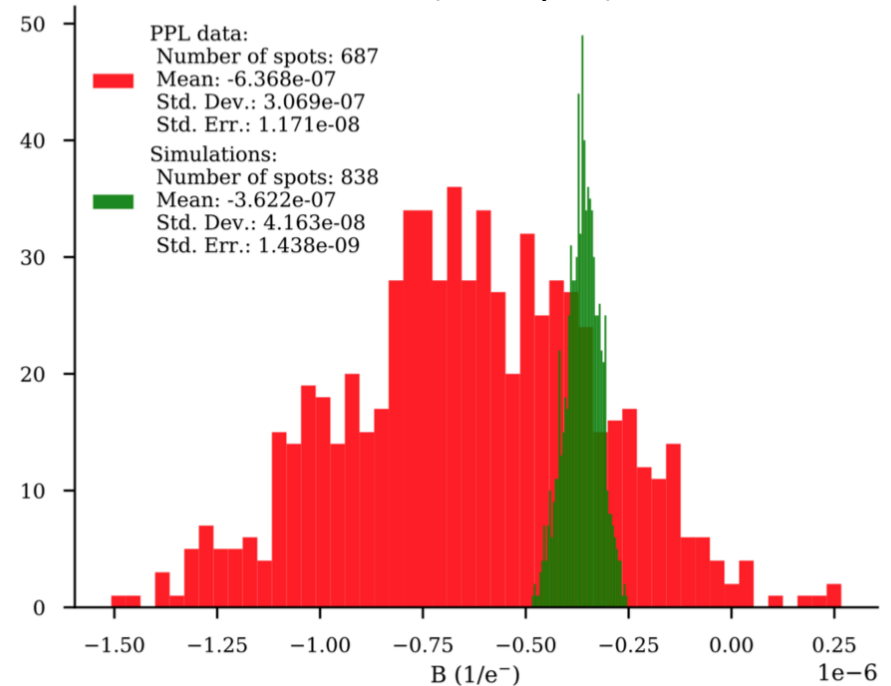
B = (dA/A) / Q_c = pixel area change per e− of contrast

→ B ~ 1E-6 with variations not explained by noise

$$Q_c = Q_{\text{central}} - (Q_{\text{left}} + Q_{\text{right}} + Q_{\text{top}} + Q_{\text{bottom}})/4$$
$$Q_c = F_c t$$

Y-band (1 µm)

PPL data:
  Number of spots: 707
  Mean: -1.103e-06
  Std. Dev.: 3.425e-07
  Std. Err.: 1.288e-08
Simulations:
  Number of spots: 838
  Mean: -3.622e-07
  Std. Dev.: 4.163e-08
  Std. Err.: 1.438e-09

H-band (1.55 µm)

PPL data:
  Number of spots: 687
  Mean: -6.368e-07
  Std. Dev.: 3.069e-07
  Std. Err.: 1.171e-08
Simulations:
  Number of spots: 838
  Mean: -3.622e-07
  Std. Dev.: 4.163e-08
  Std. Err.: 1.438e-09

Brighter-fatter test conclusions

- There is a clear difference between the nonlinear response of flats and spots (at 1μm, 1.55μm)

- After NL calibration, bright spot centers lose flux, neighbor pixels gain flux, but flux is not conserved

- Non-linear IPC is likely in play (see work by Donlon): maybe NL-IPC explains missing flux. NL-IPC tests using single pixel reset would be valuable

- Other possible BF tests:

  - selective reset (project images onto "pre-filled" pixel patterns)

  - superimposing flats/spots

  - Galaxy shapes instead of stars

Crosshatch Analysis

- Engineering grade H2RG (#18546) was lent to JPL to investigate nature of the cross-hatch pattern seen in flat-field images.

- Pattern is visible even under an optical microscope. Manifestation of defects in the HgCdTe crystal.

- Concern: this "feature" may correspond to sub-pixel variations in quantum efficiency (QE) or charge redistribution (like "tree rings" in Dark Energy Survey), making photometric calibration difficult.

- By emulating Euclid-like point sources, we can measure the nature of this pattern and what effect it has on photometry
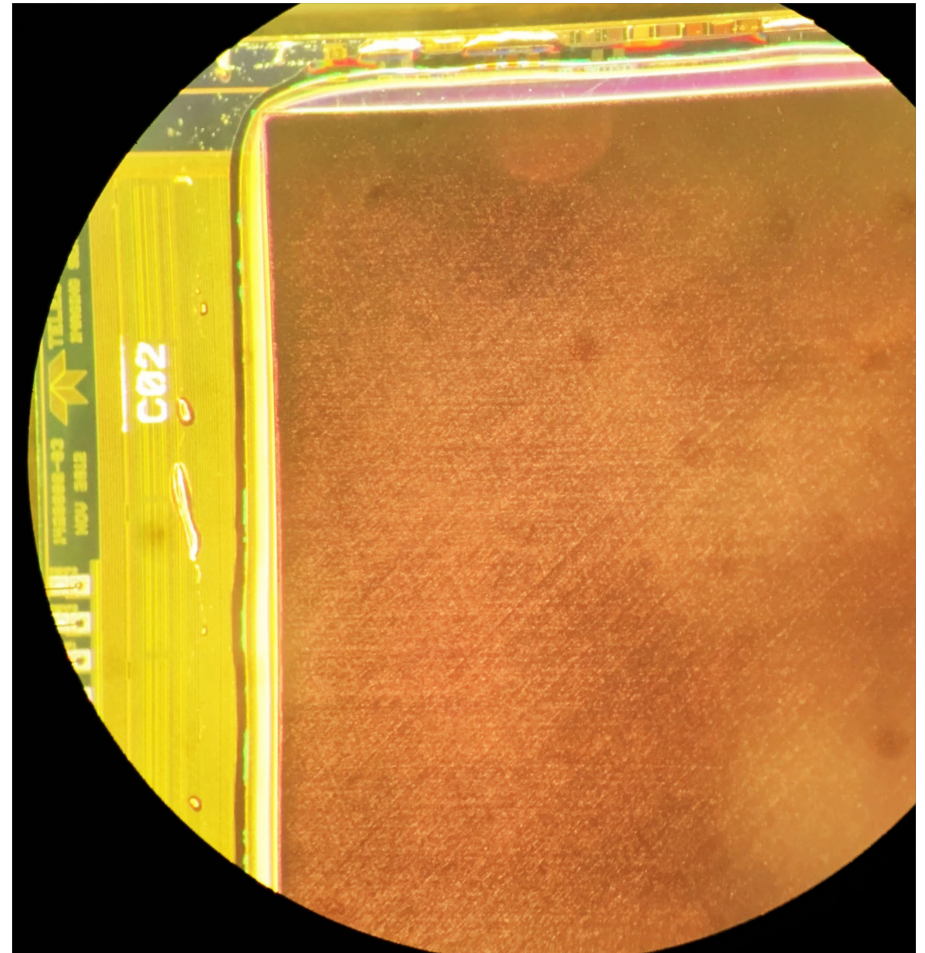
Image of H2RG #18546 taken with iPhone held up to microscope

Cross-hatch pattern in flat field (λ=1µm)

Diffuse image at ~1µm. Contrast adjusted to emphasize cross-hatch.
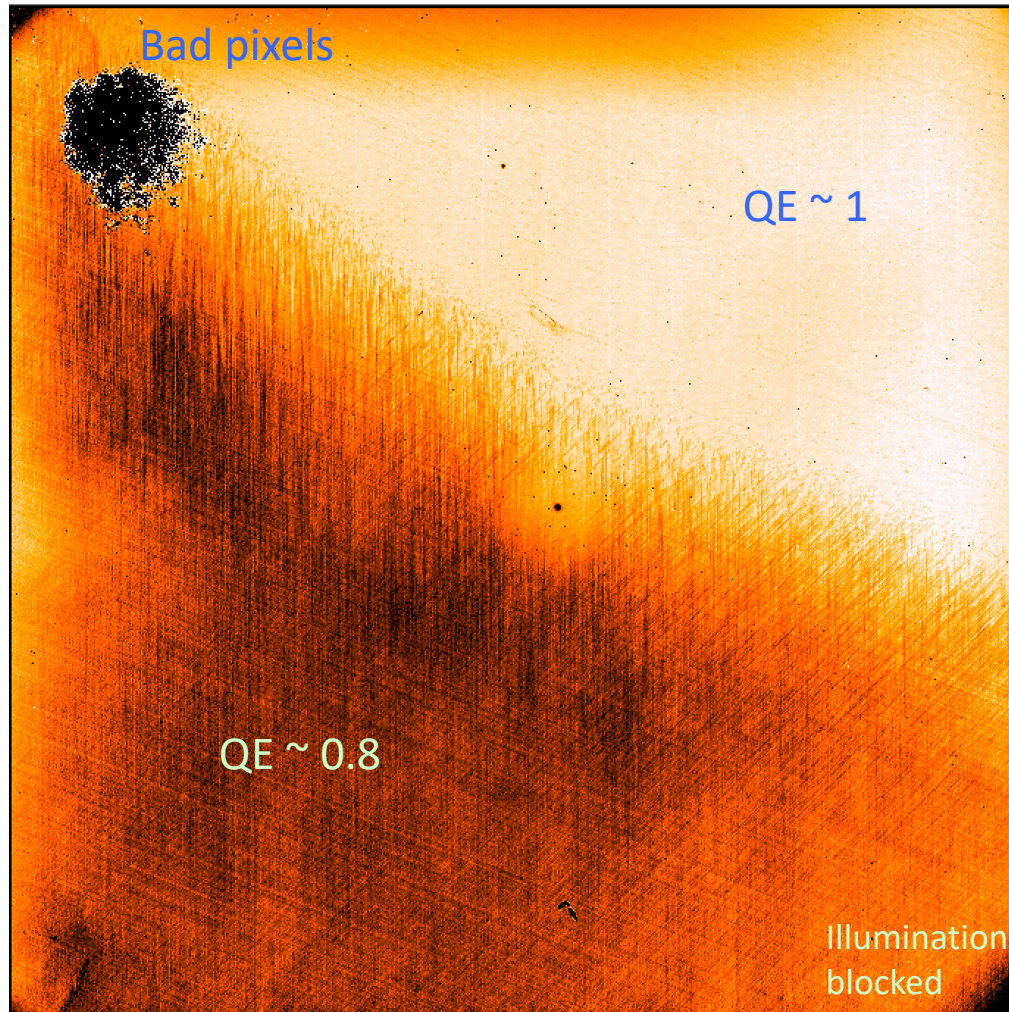
- Euclid flight detectors look like the upper region with **less** cross-hatching.

Power spectra of "weak" and "strong" crosshatch regions – 1µm
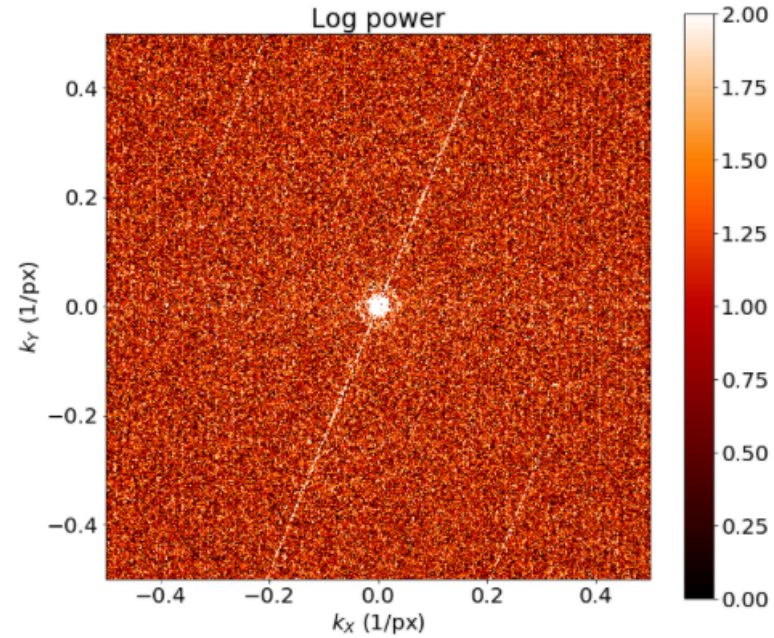

Aliased power ($k > k_{Nyquist}$)
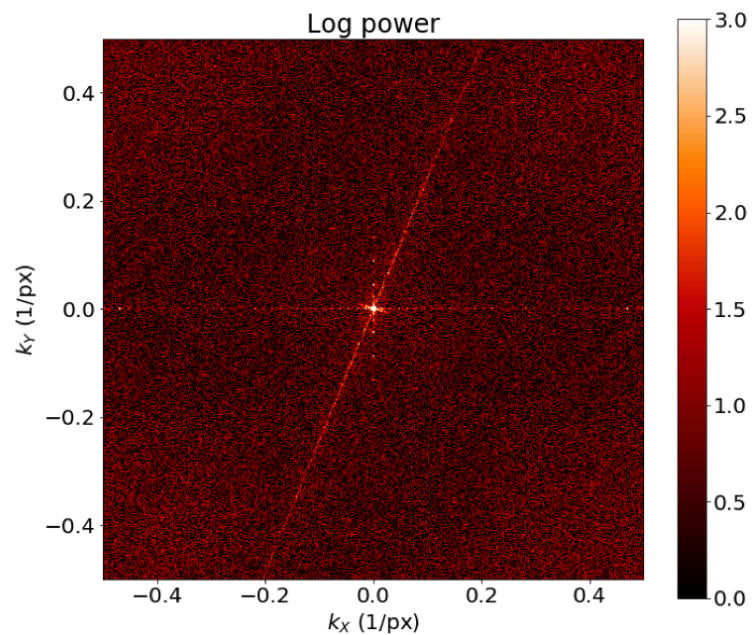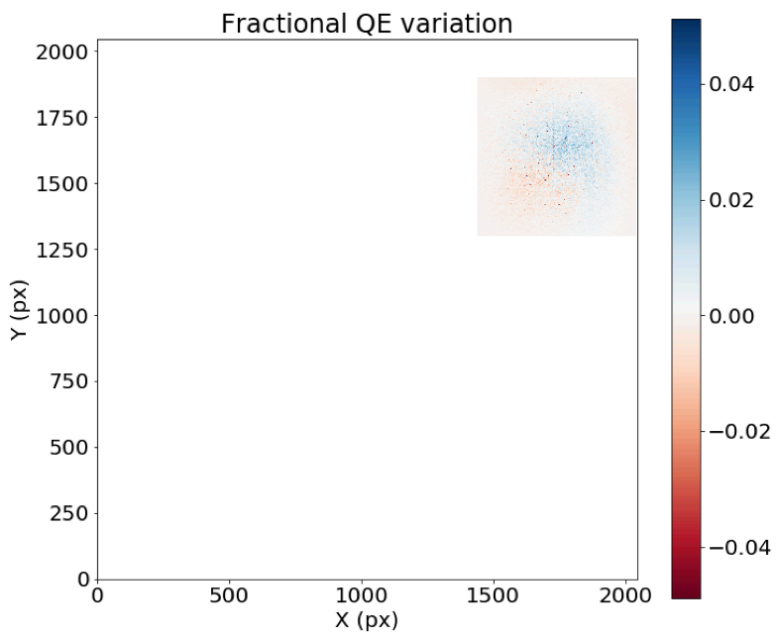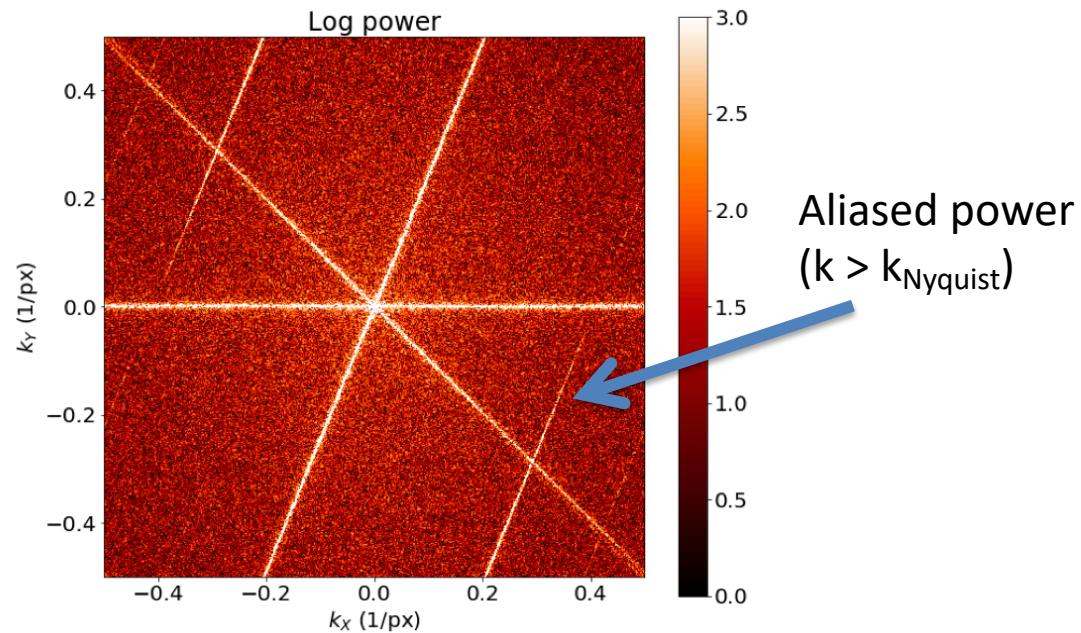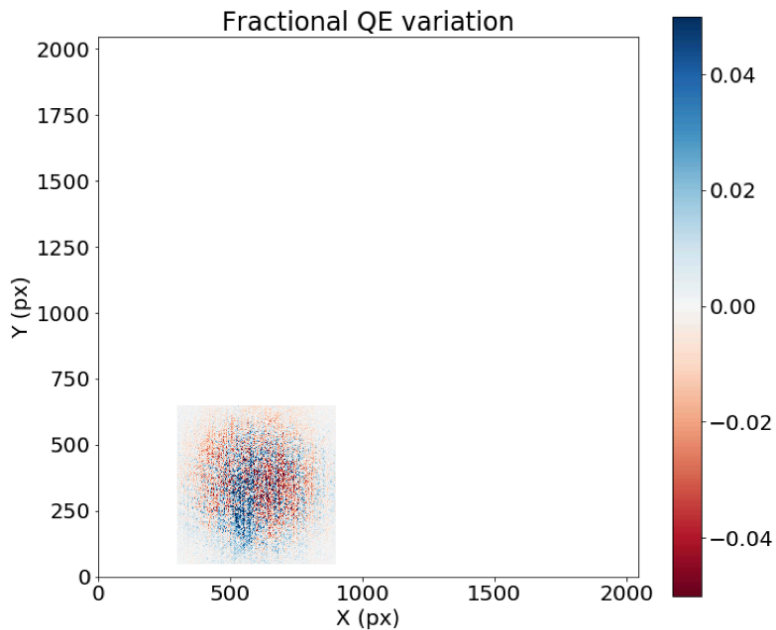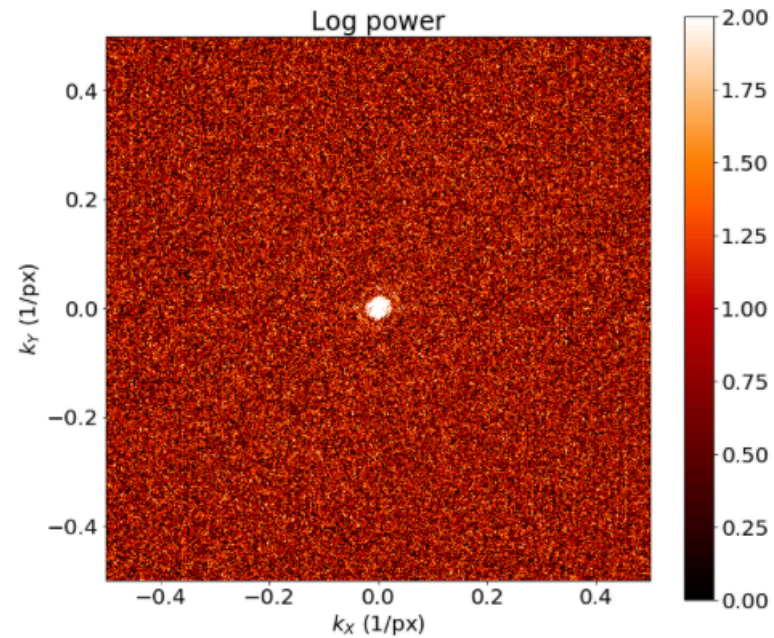
Power spectra in "weak" and "strong" crosshatch regions – 1.55μm
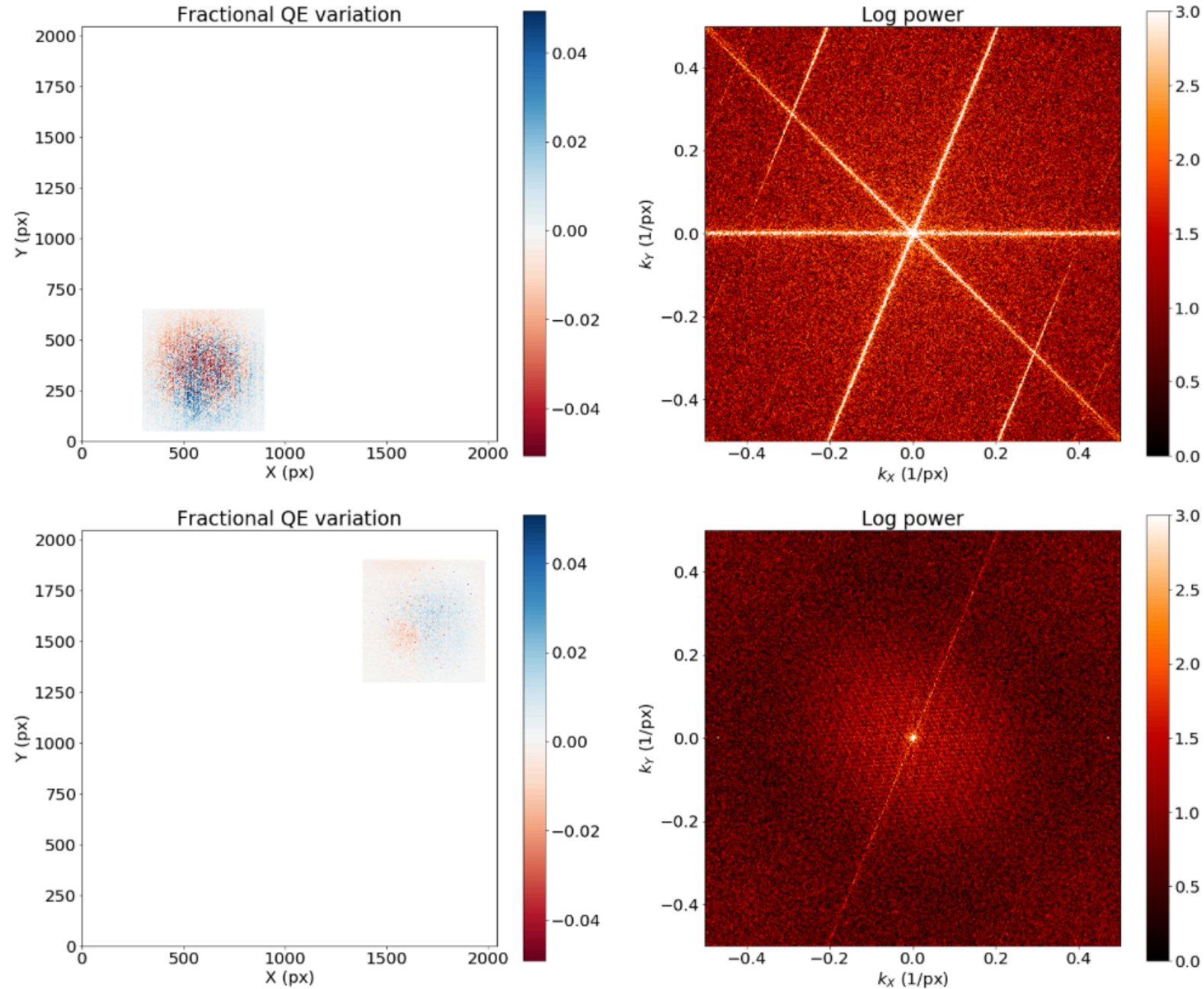
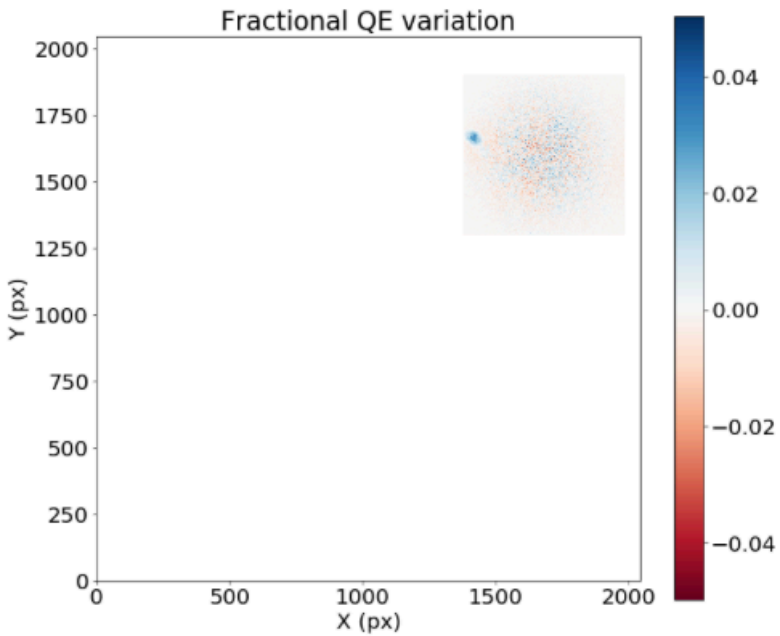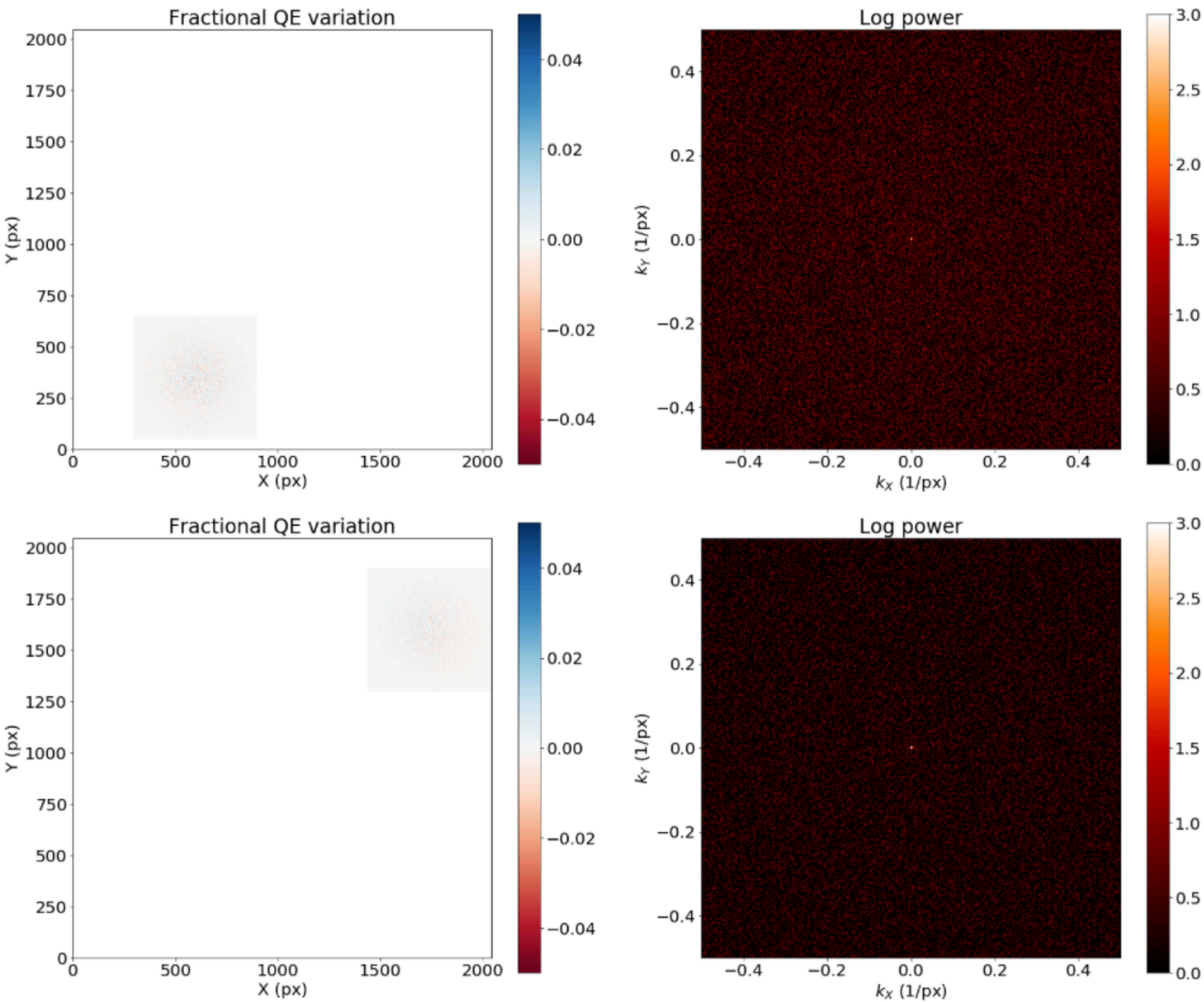# Power of ratio of 1μm and 1.55μm flats
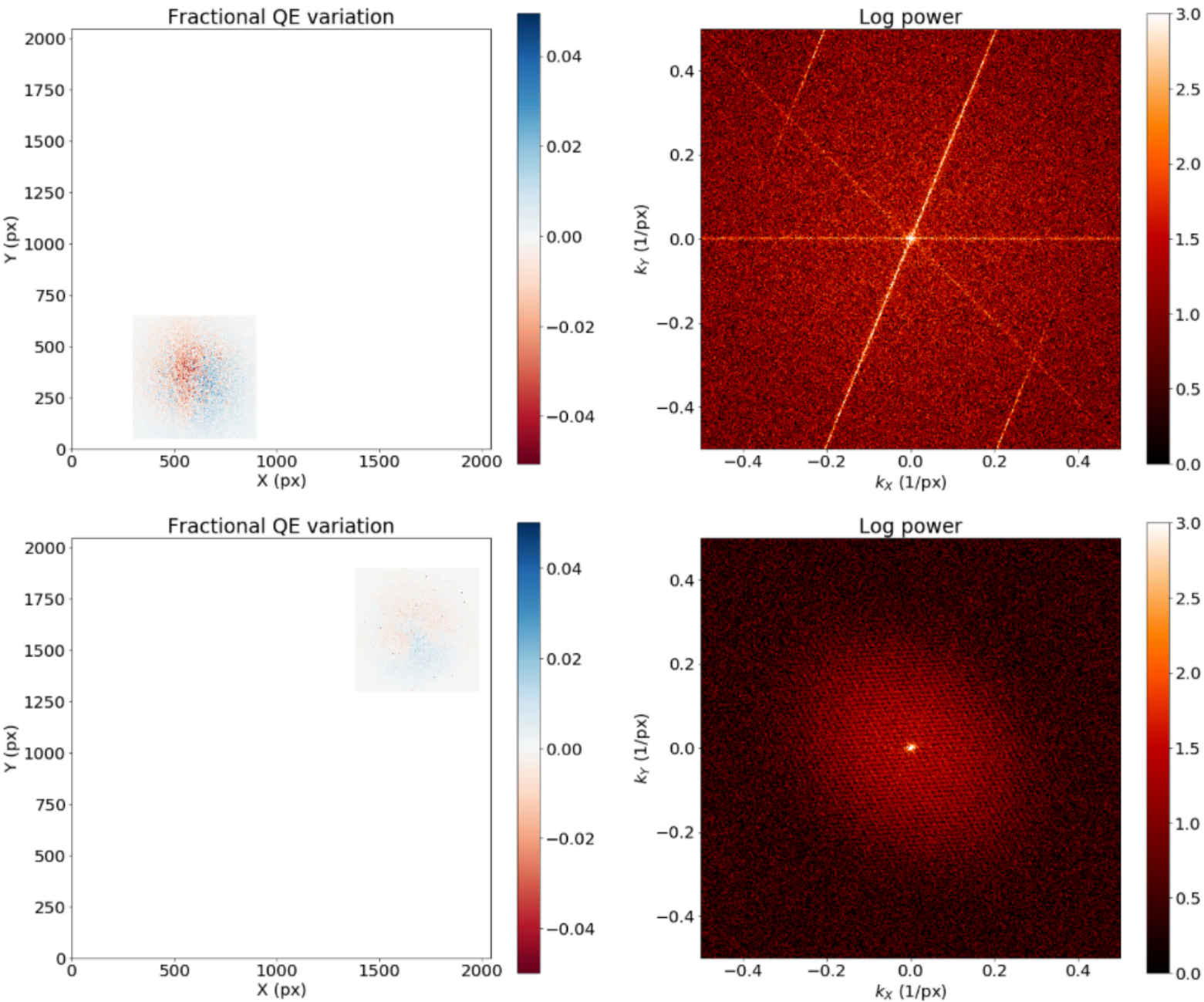
Power of ratio of f/11 and f/44 flats (1μm)
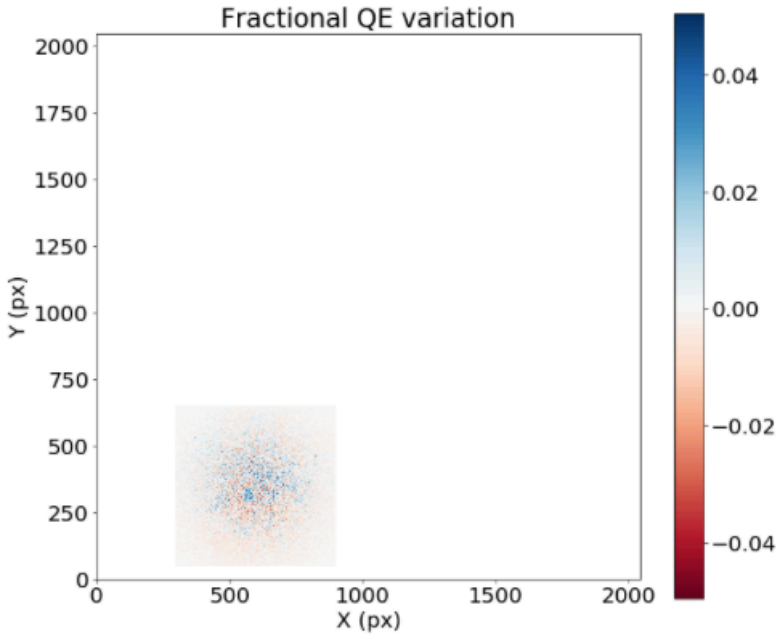
Hint of dependence on angle of incidence

Power of Ratio of flats with 2 orthogonal polarization filters **on source**

Sub-pixel Spot scanning

- Same setup as for brighter-fatter tests

- Spot grid was raster scanned in 6μm steps (1/3 pixel). 6μm is about the resolution limit of the Y-band PSF at f/11. Relative positions are accurately measured by averaging all spot centroids.

- Calibrations applied to images: dark subtraction, flat fielding, conversion gain, pixel-wise nonlinearity, discarding data near "bad" (outlier) pixels

- Detrending removes any lamp variations

- Not corrected: IPC, persistence

- When mapping QE, scan pattern was interlaced so that spots do not overlap previous exposures (avoids persistence)

- Analyze aperture photometry vs. position
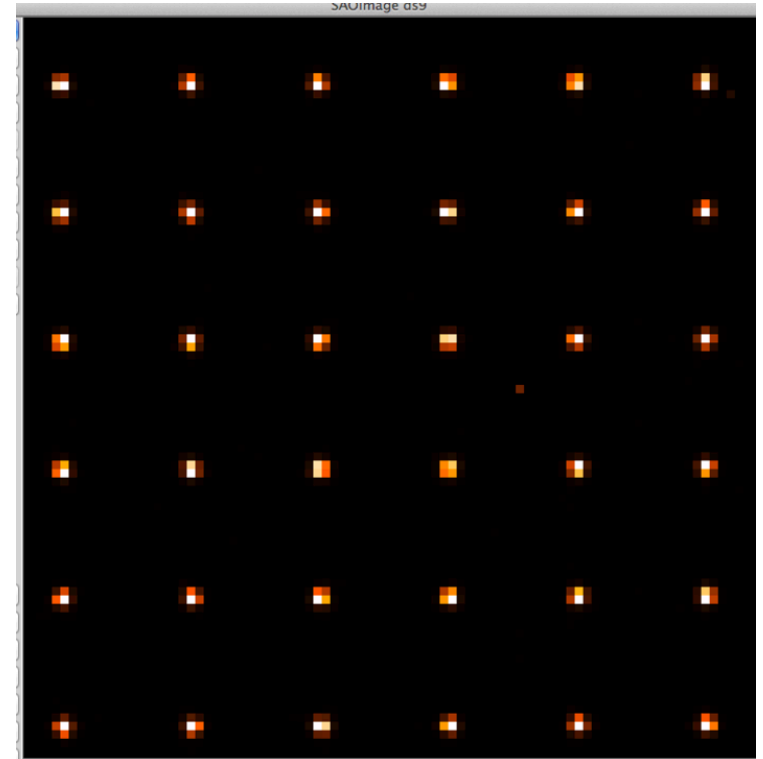
Spot grid focused on 90x90 pixel region of H2RG #18546

Photometry Degradation due to small image translations (Y-band)

- In a calibrated detector, photometry should not vary with position. Flat-fielding suppresses QE variations larger than 1 pixel but will not remove sub-pixel variation.

- We map the difference in scatter (σ/**mean**) for individual spot fluxes over sequences of scanned images at different positions ("moving") or at the same position ("fixed").

- **"Fixed"** sequence = 9 images at same position

- **"Moving"** sequence = 10 images in 1/3 pixel steps; spans 3 pixels
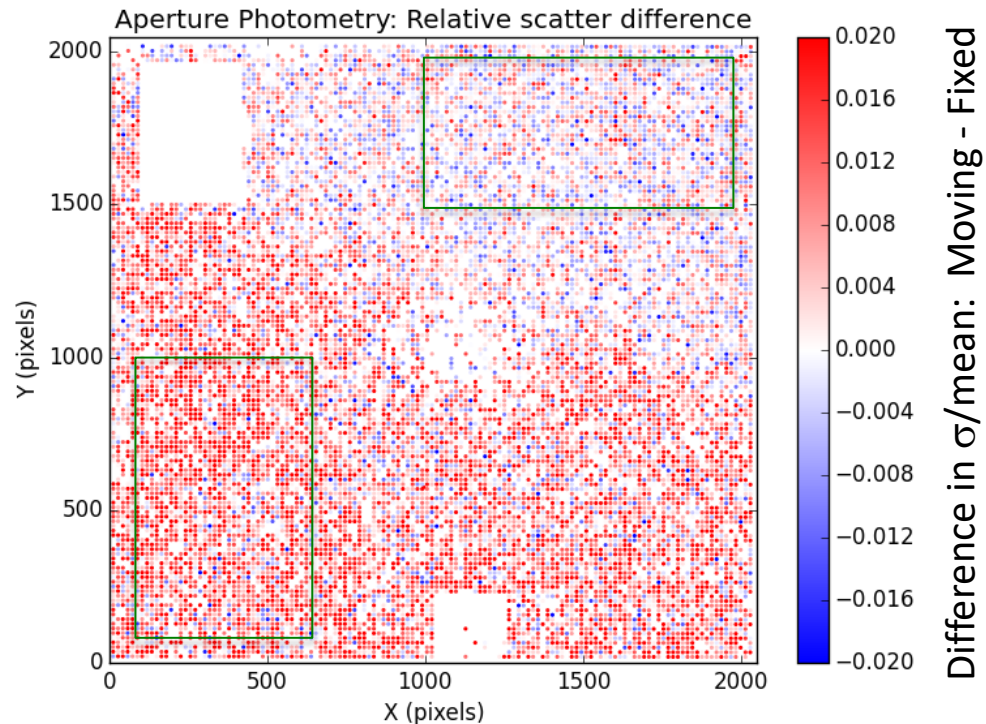
$\Delta(\sigma/\text{mean})$ averaged over large regions:

WEAK Crosshatch: 0.0002 ± 0.0006
STRONG Crosshatch: 0.010 ± 0.0005

Photometry Degradation due to small image translations (H-band)

- H band version of this particular test was **inconclusive**

- We tried new masks with 4x more spots to speed up data acquisition. Later discovered that new masks were not fully opaque to NIR. (much higher background noise)
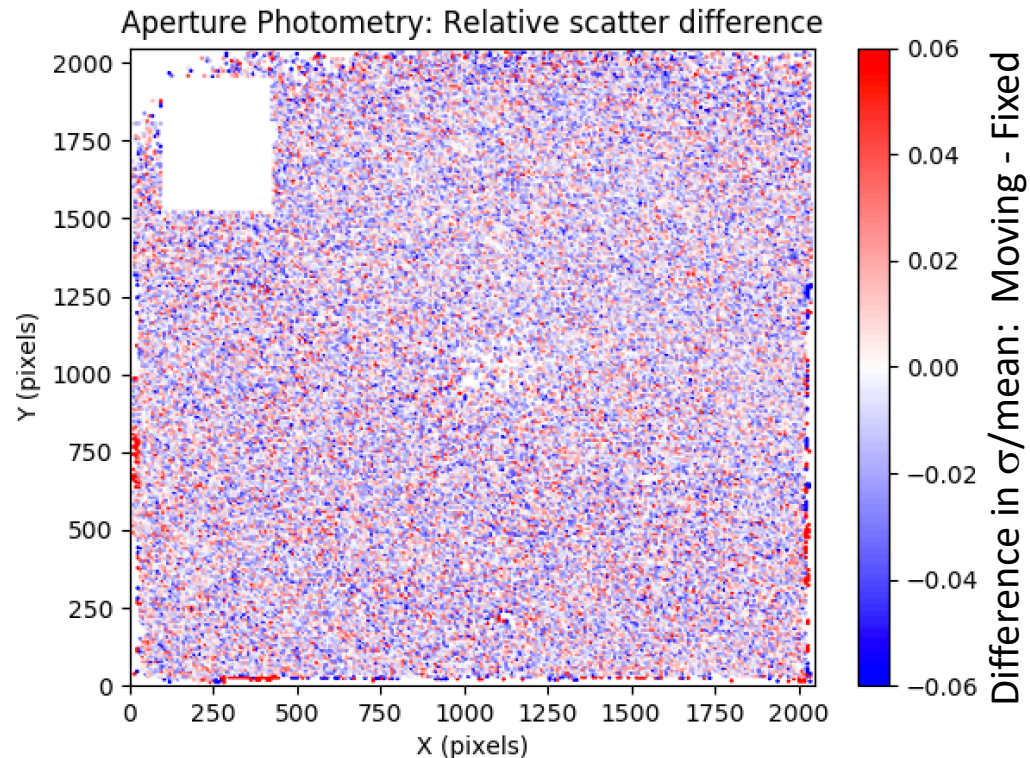
Statistics of σ/mean per spot in "Fixed" image after sigma-clipping (4 sigma):

Y-Band (good mask)
- MEAN 0.029
- STDDEV 0.0081

H-band (bad mask!)
- MEAN 0.069
- STDDEV 0.013

We can of course repeat this if needed

Aperture Photometry: Relative scatter difference

Averages over large regions are consistent with noise

Interpretation

- Scanning the spots over 3 pixels has no significant effect on photometric stability in the good detector region. Scatter in the cross-hatched region increases by 1.5% relative to mean. Flat fielding reduces this to 1%.

- This is consistent with sub-pixel QE variations along the scan (column) direction. Photometry is measured by summing all pixels in an aperture; if the cross-hatch pattern were due to charge redistribution, we expect no effect in the uncorrected images, and flat fielding would make the photometry worse.
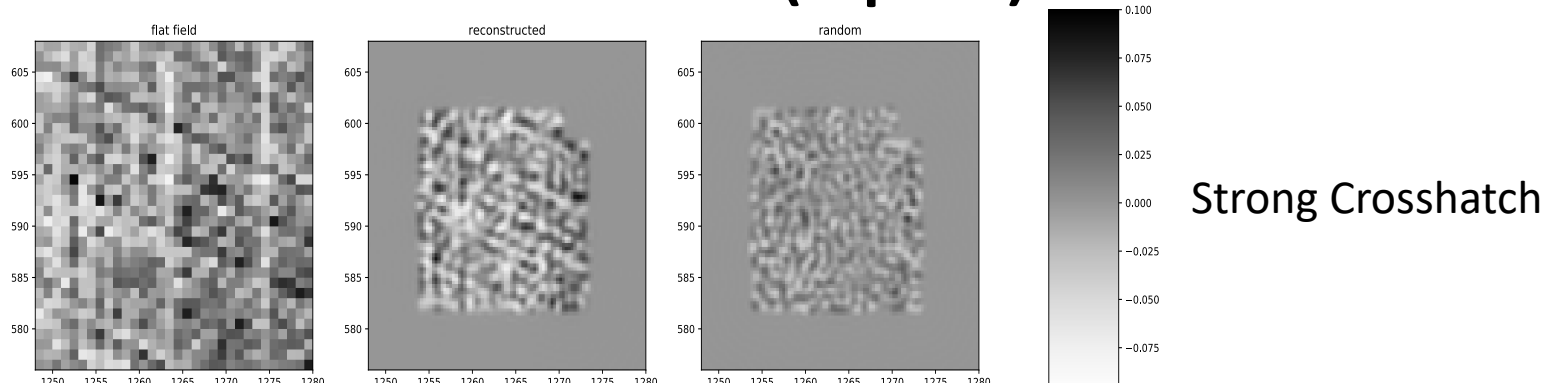
Optimal Linear Interpolation
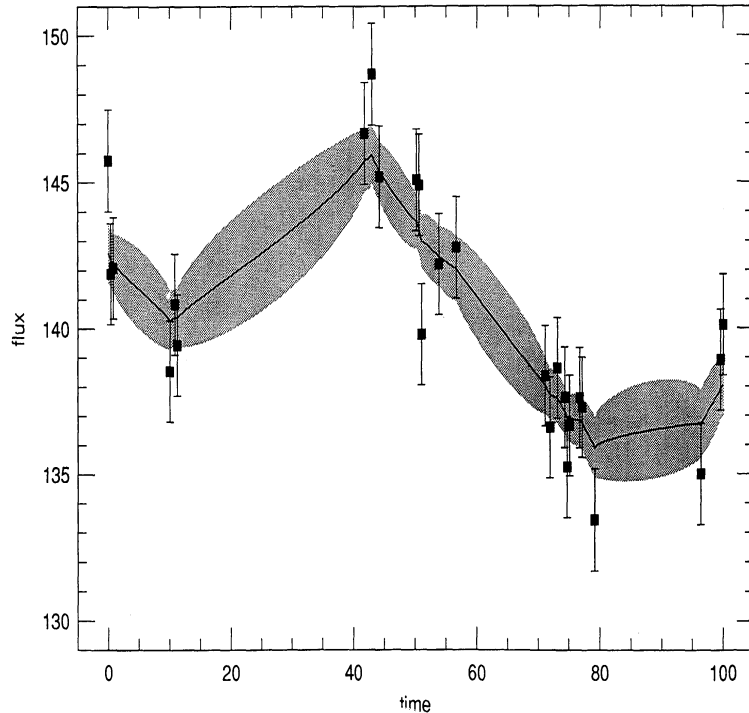
- We construct a Wiener filter using the known noise (**N)** and signal (**S**) covariances
- **S** is set by the PSF, modeled here as an Airy function
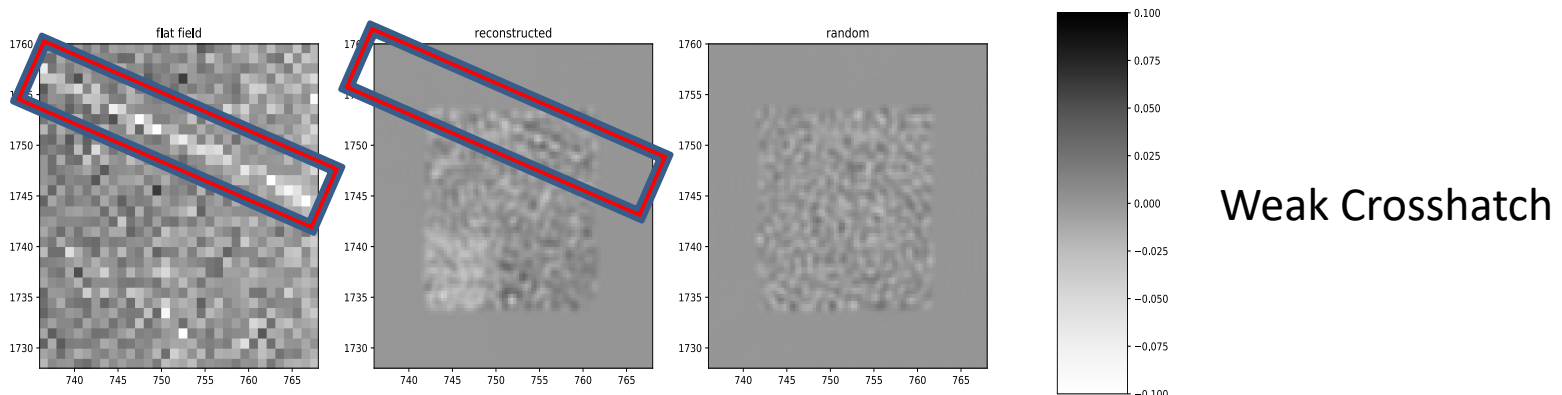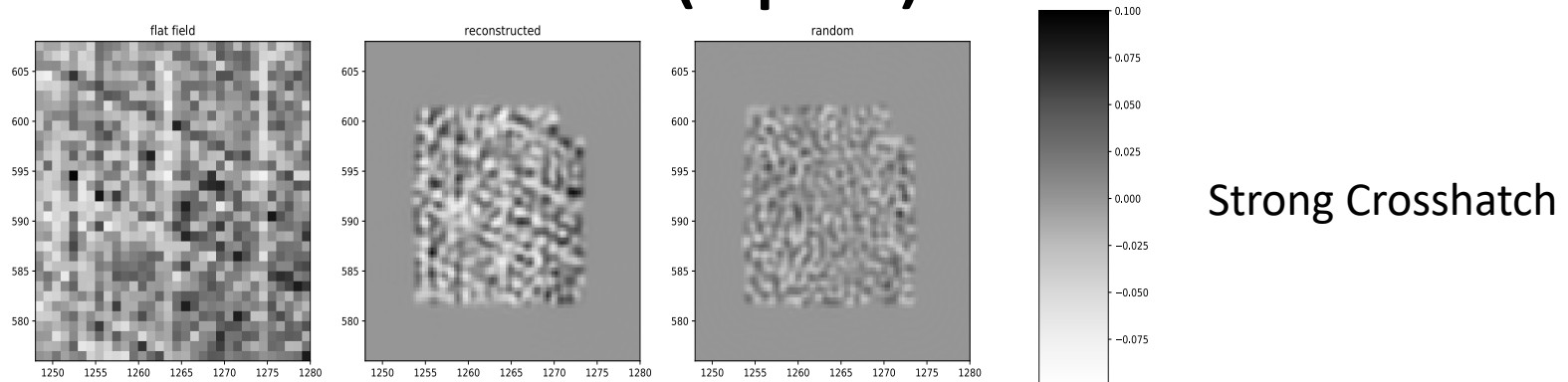- We interpolate the spot photometry onto a 3x3 subpixel grid in

$$\hat{p} = S_\times \left[S + N \right]^{-1} \left(d - \bar{d} \right) + \bar{d}$$

The pattern does not flat field away. (1μm)

Strong Crosshatch
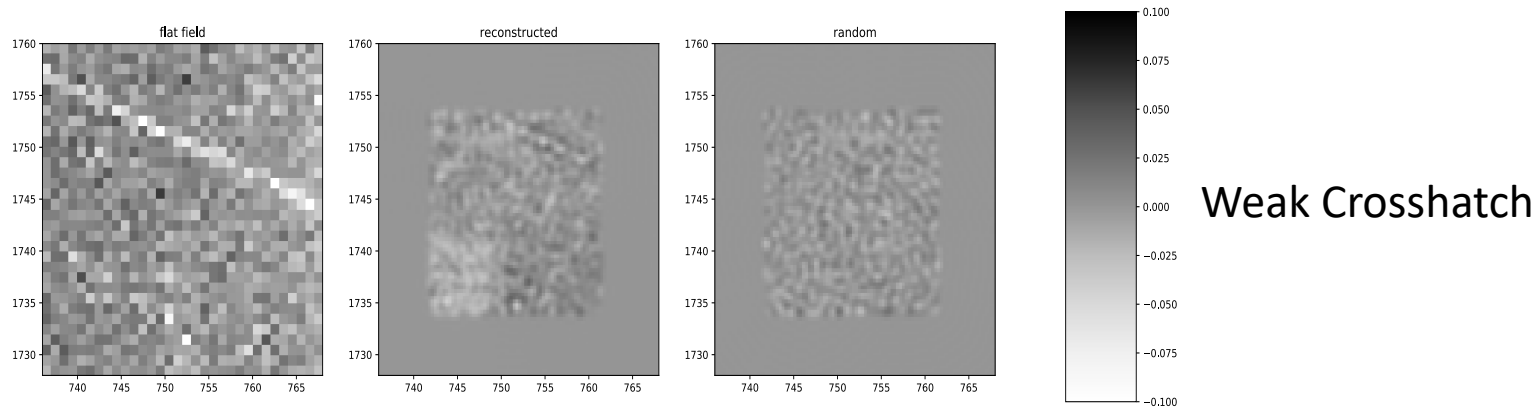
Weak Crosshatch

The spot photometry is 1.3% noisier in the strongly crosshatched region.

The pattern does not flat field away. (1μm)
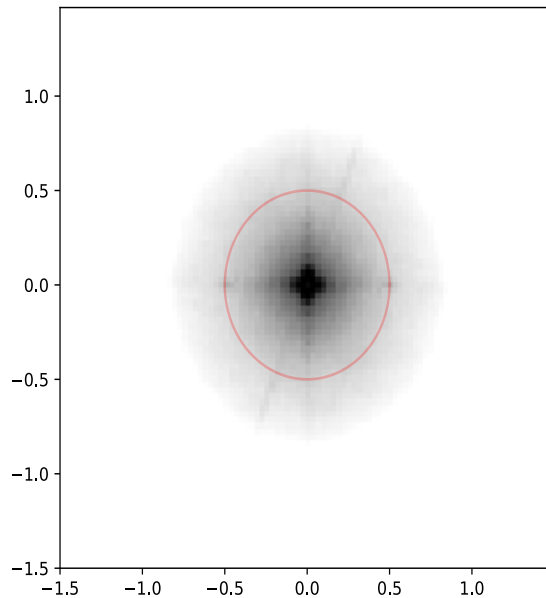

Strong Crosshatch

Weak Crosshatch

- The spot photometry is 1.3% noisier in the strongly crosshatched region.

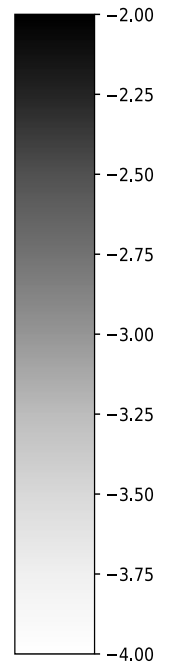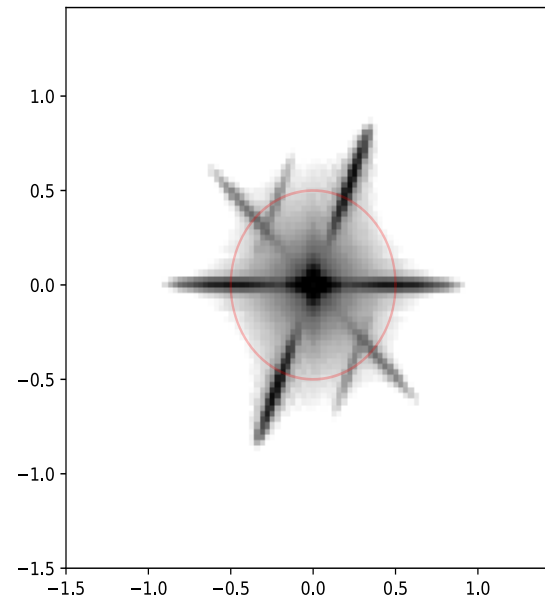- Even in the weak region, isolated stripes are not removed

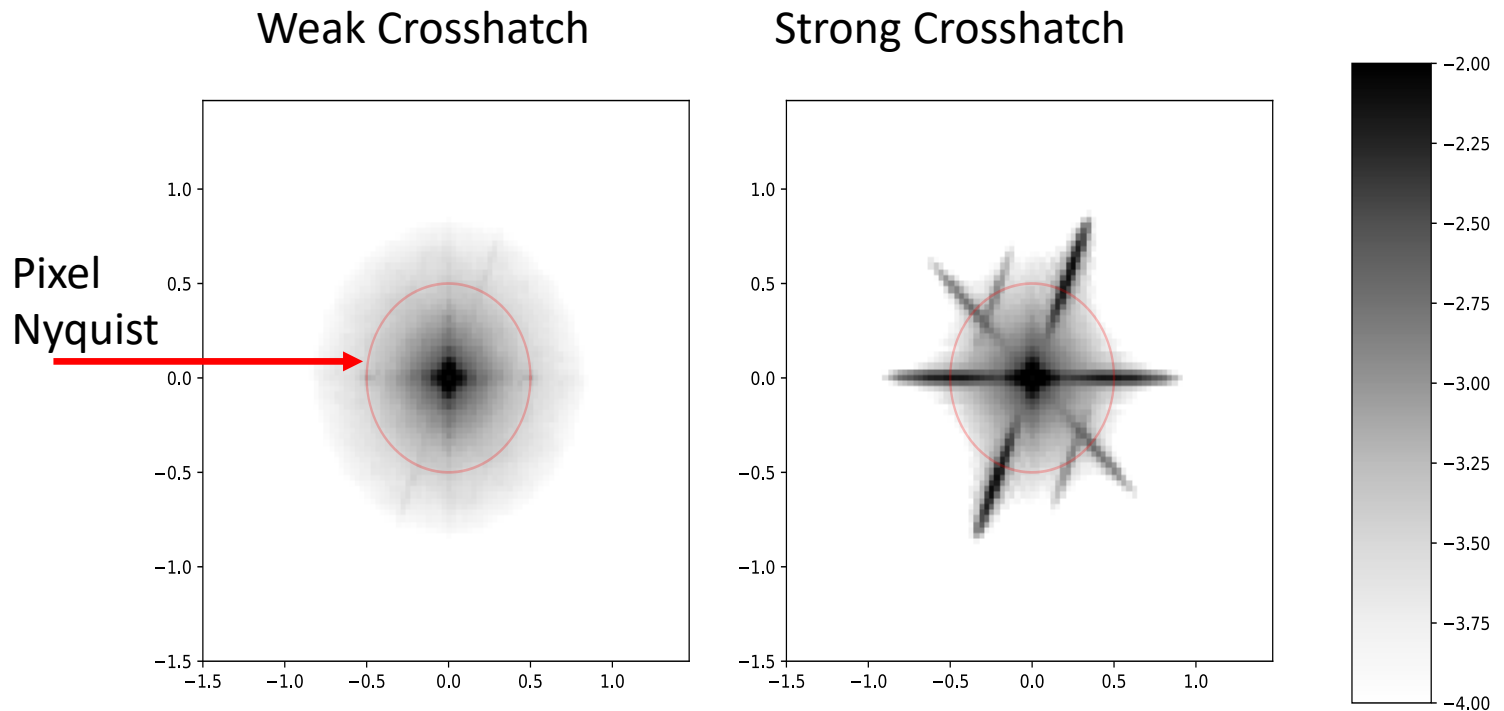# We then calculate the power spectrum of the reconstructions.

We then calculate the power spectrum of the reconstructions. (1μm)
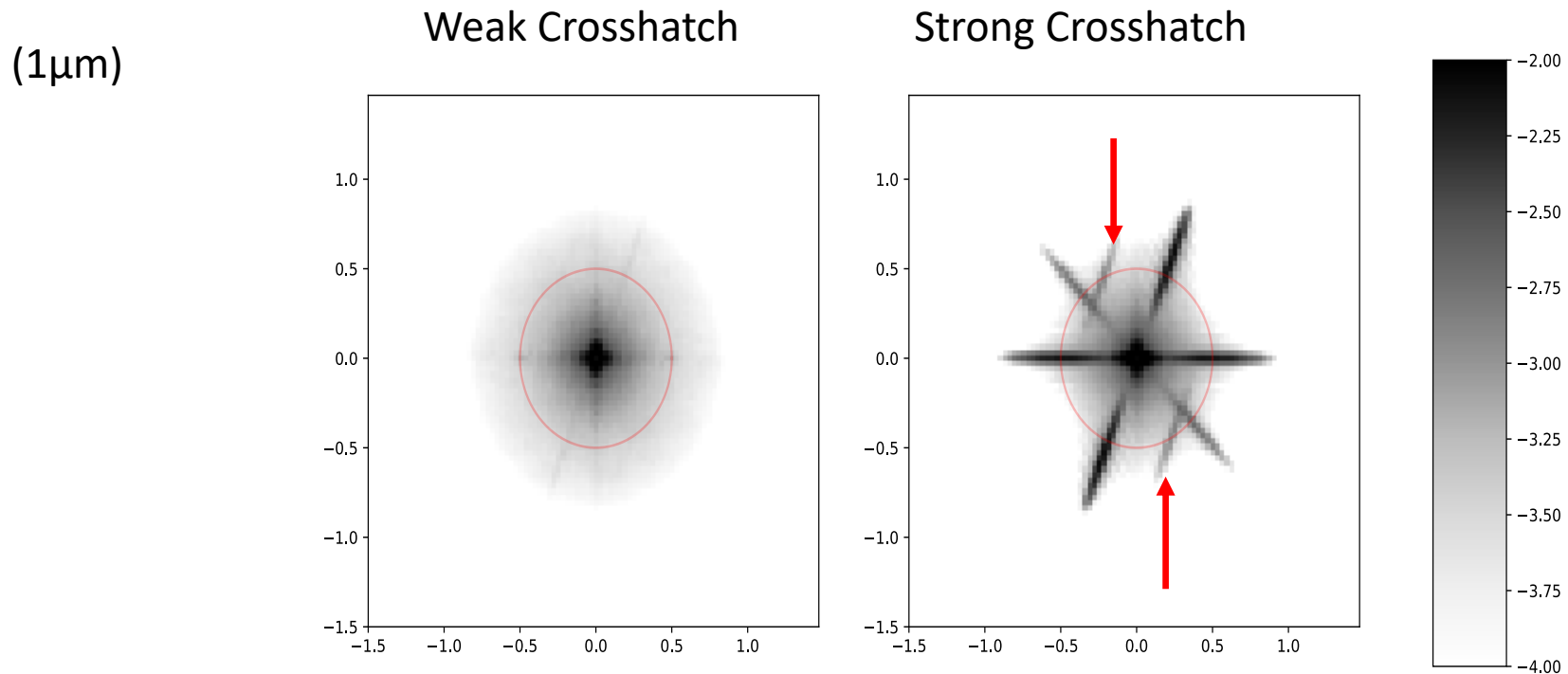
(1μm)

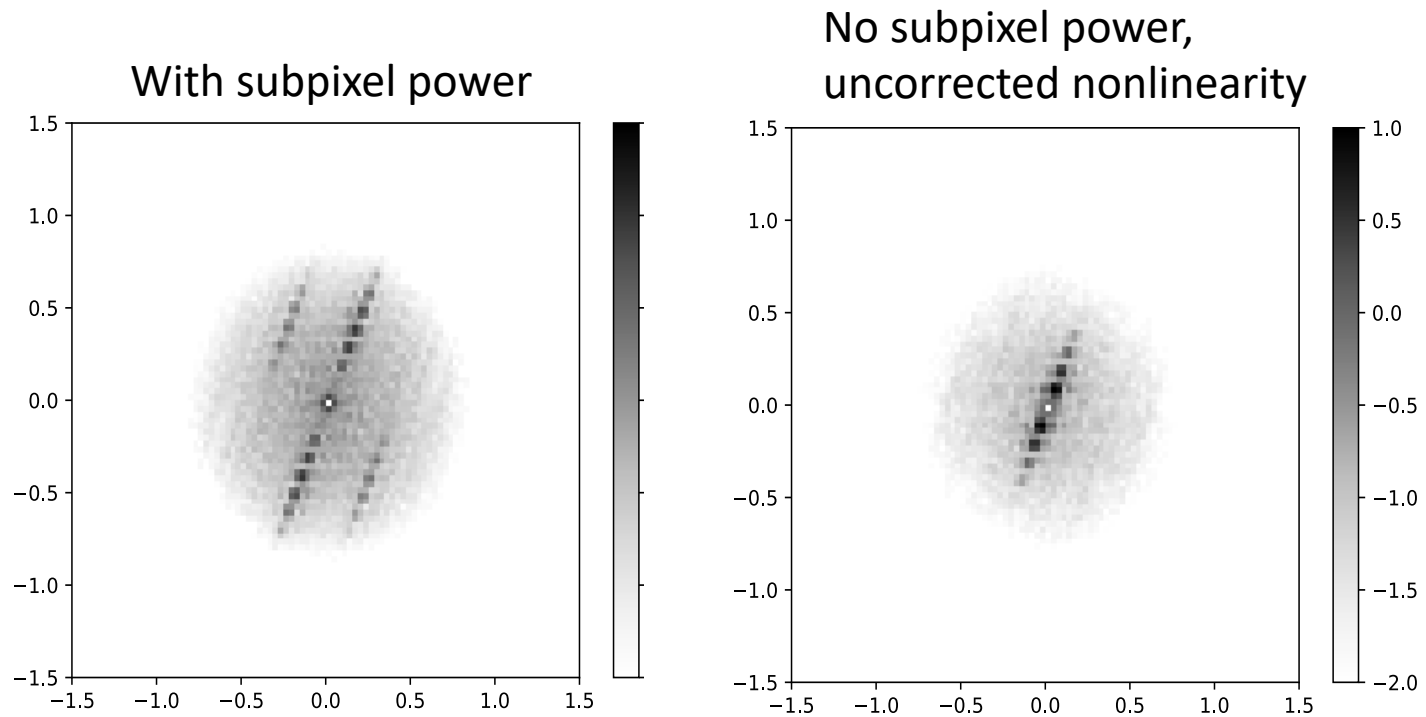Weak Crosshatch

Strong Crosshatch

Pixel
Nyquist

# We then calculate the power spectrum of the reconstructions.

High-frequency power, oriented along crosshatch pattern.
The folded spikes may be aliased higher-frequency power.

We simulated sub-pixel power and its impact on photometry.

With subpixel power

No subpixel power,
uncorrected nonlinearity

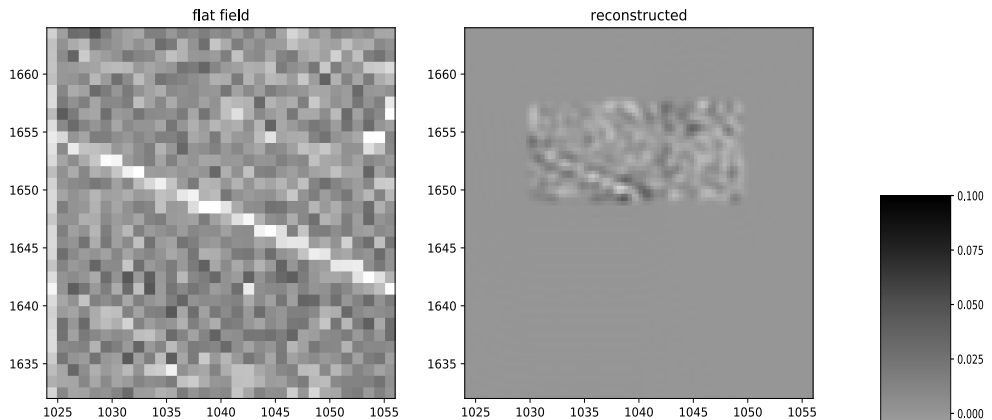We are unable to reproduce the 'folded' spikes without adding subpixel power.

We then repeated the experiment in the H-band (1.55 μm)
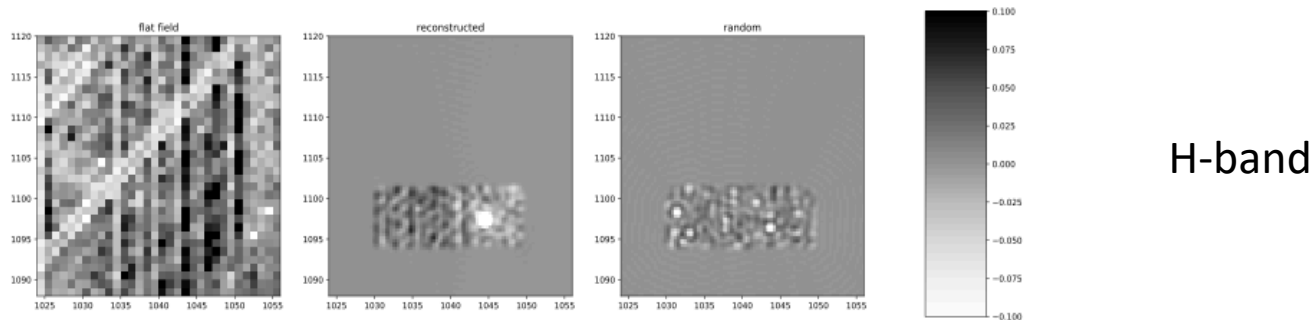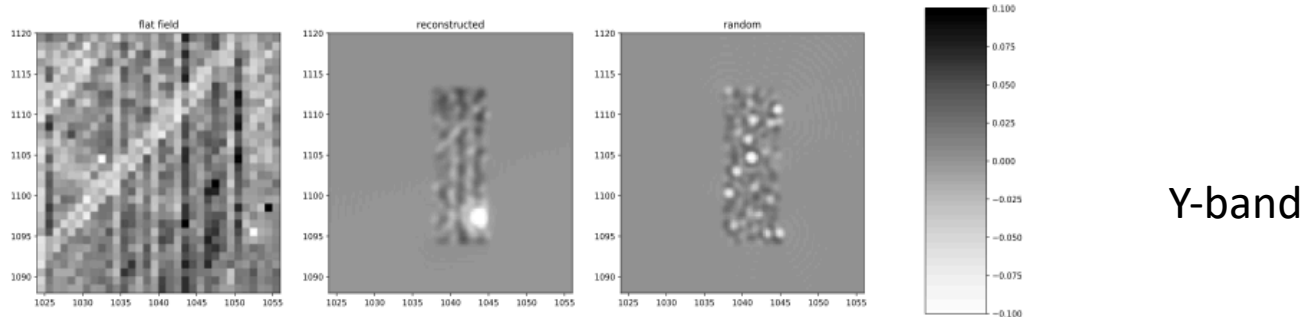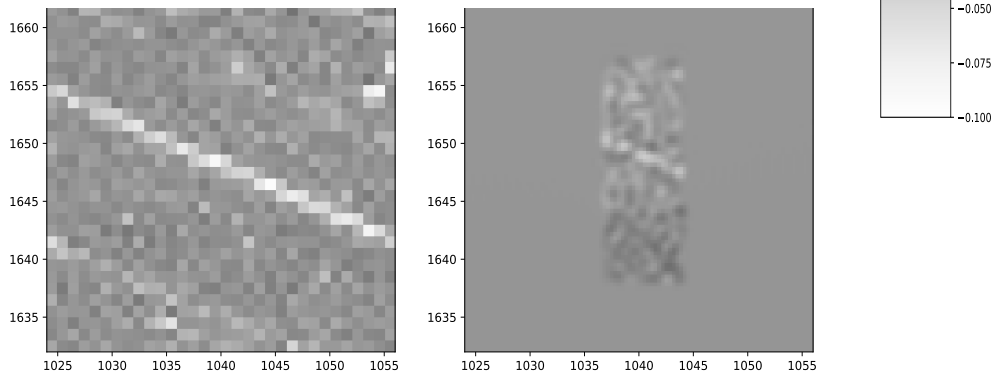

Y-band

H-band

The subpixel features remain, but the excess power in strong region is reduced to 1% (as opposed to 1.3% in Y).

Residual systematics in the weak region:

Peak deviation
Y-band: +/- 0.042
H-band: +/- 0.035

H-band sees a quantitative reduction in residual power of **tens of percent**.

- We see strong evidence that crosshatching is due to sub-pixel QE modulation.

- We qualitatively reproduce patterns from our data with simple simulations.

- We have now made measurements in both Y and H-bands. These are consistent, but with H suppressed by ~10s of per cent.

- The maximum variation in the presence of crosshatching is 3% - 4%.